

Article

Geochemical Partitioning of Heavy Metals and Metalloids in the Ecosystems of Abandoned Mine Sites: A Case Study within the Moscow Brown Coal Basin

Ivan Semenov ^{1,*}, Anna Sharapova ¹, Sergey Lednev ¹, Natalia Yudina ¹, Andrey Karpachevskiy ¹, Galya Klink ² and Tatiana Koroleva ¹

¹ Faculty of Geography, Lomonosov Moscow State University, 119991 Moscow, Russia; avsharapova@mail.ru (A.S.); sled1988@mail.ru (S.L.); natttally7@gmail.com (N.Y.); karpach-am@yandex.ru (A.K.); korolevat@mail.ru (T.K.)

² Institute for Information Transmission Problems (Kharkevich Institute) of the Russian Academy of Sciences, 127051 Moscow, Russia; galkaklink@gmail.com

* Correspondence: semenkov@geogr.msu.ru

Abstract: Significant environmental impacts of mining activities connected with high-sulfur materials result from the production of acid mine drainage and potentially toxic elements, which easily migrate to adjacent ecosystems due to the typical absence of vegetation on spoil heaps and toeslope talus mantle. In this paper, we present the results of the first comprehensive study of the ecosystems affected by acidic and metal-enriched (Al, Ca, Co, Cu, Fe, Mg, Mn, Ni, and Zn) mine drainage conducted at spoil heaps and adjacent talus mantle under semihumid climate conditions within the Moscow Brown Coal Basin (Central Russian Upland, Tula Region, Russia). A total of 162 samples were collected, including 98 soil samples, 42 surface water samples, and 22 plant samples (aerial tissues of birch). Coal talus mantle materials of Regosols were characterized by the increased concentration of water-soluble Ca, K, Mg, and S, and all mobile fractions of Al, Co, S, and Zn. The chemical composition of birch samples within the zones affected by acid mine drainage differed insignificantly from those in the unpolluted ecosystems with black soils, due to the high tolerance of birch to such conditions. Differences between the affected and undisturbed sites in terms of the chemical composition decreased in the following order: waters > soils > plants. The geochemical characterization of plants and soils in coal mining areas is essential for the mitigation of negative consequences of mining activities.

Keywords: acid mine drainage; black soils; coalmine waste; potentially toxic elements; chemical speciation; water pollution; waste-rock dumps; tailings pond; mine tailings; translocation factor; mining soils



Citation: Semenov, I.; Sharapova, A.; Lednev, S.; Yudina, N.; Karpachevskiy, A.; Klink, G.; Koroleva, T. Geochemical Partitioning of Heavy Metals and Metalloids in the Ecosystems of Abandoned Mine Sites: A Case Study within the Moscow Brown Coal Basin. *Water* **2022**, *14*, 113. <https://doi.org/10.3390/w14010113>

Academic Editor: David Widory

Received: 21 November 2021

Accepted: 29 December 2021

Published: 5 January 2022

Publisher's Note: MDPI stays neutral with regard to jurisdictional claims in published maps and institutional affiliations.



Copyright: © 2022 by the authors. Licensee MDPI, Basel, Switzerland. This article is an open access article distributed under the terms and conditions of the Creative Commons Attribution (CC BY) license (<https://creativecommons.org/licenses/by/4.0/>).

1. Introduction

Up to the present time, coal remains a main energy source in the power supply systems of many countries around the world, despite the fact that its carbon footprint is high [1,2]. The coal mining industry negatively affects the environment by high water consumption, pollution of the hydrosphere [3] and the atmosphere [4,5], loss of agriculturally valuable lands [6], and damage to the quality within areas of coal-mine waste disposal [7,8]. In particular, degradation of ecosystems occurs under the impact of acid mine drainage, which is generated due to the oxidation of sulfides in spoil heaps and the mobilization of potentially toxic elements [9]. All these factors create health risks to residents of nearby settlements [10] and employees of coal mines [11]. Similar problems are associated with dumps of wastes of other sulfide-rich raw materials around the world [12,13], as well as areas with acid sulfate soils [14] and thermal acid sulfate waters within recent volcanic activity zones [15].

In Russia, there are 22 coal basins with 129 separate deposits of coal [16]. At the beginning of 2021, active coal mining was recorded in 58 shafts and 121 quarries [17]. The first studies on the ecological consequences of dumping sulfide-rich coal-mine waste without mitigation were conducted under the supervision of N.P. Solntseva in the 1970s in the former Soviet Union, within the Kizel Brown Coal Basin [18] and further within the Moscow Brown Coal Basin [19,20] where coal bearing rocks are rich in sulfur compounds. The Kizel Brown Coal Basin studies [18] demonstrated for the first time that coal mining results in soil contamination by heavy metals and metalloids (HMMs), which originate from waste rocks, and described the main processes of the formation of technogenic leakage fluxes that cause secondary pollution by Cd, Pb, and Zn. Those studies highlighted the importance of sulfur as a typomorphic element, which migration characterizes a given epigenetic process [21] and predetermines the geochemical specificity of landscapes and the formation of anomalies in coal mining areas. Such geochemical anomalies are especially damaging for pedalfers (acid soils) of humid regions due to their low buffer capacity, which is predetermined by a low cation exchange capacity and a low base saturation. Concentration levels and distribution patterns of different sulfur compounds (sulfates, sulfides, and organic and free S) can serve as indicators of the intensity of soil pollution and the durability of its consequences. For example, in the northern and central parts of the East European Plain, the prevalence of sulfates in soil indicates the soil's capability from self-remediation from S compounds. High proportions of low-valent compounds (iron sulfide and free S) under reductive conditions indicate the formation of man-made anomalies. Secondary sulfides produced under anaerobic conditions decrease the toxicity of many HMMs by forming insoluble substances. In cases of remediation of such potentially acid soil, these sulfide anomalies generate serious risks of secondary environmental pollution due to the oxidation of newly formed sulfides and the mobilization of potentially toxic Al, Cd, Cu, Mn, Pb, Zn, and other elements [22].

Despite the high extractability of HMMs from pedalfers, these soils have a low potential for self-remediation from high concentrations of HMMs due to their accumulation at geochemical barriers [23–25].

The Moscow Brown Coal Basin (MBCB) is situated at the southern and western borders of the Moscow syncline of the East European Craton. Over the period of the MBCB exploitation, more than 1.2 billion tons of coal have been extracted from around 180 shafts and about 100 ha of arable soils (mostly highly fertile black soils) have been lost from agriculture due to the piling up of 100 million m³ of coal-mine waste. Each spoil heap contains 300–600 thousand m³ of toxic waste rocks [26,27]. Coal mining activities within the MBCB were spontaneously discontinued in 2009, with many spoil heaps left abandoned with uncompleted remediation or without any remediation.

Adverse consequences of the abandonment of coal-mine waste, together with the generally high population of the Tula Region, have caused serious ecological problems. Non-remediated spoil heaps of the Moscow Brown Coal Basin have been studied as newly formed ecosystems evolving over time intervals of several decades [28,29], which helps to design optimal techniques for the restoration of ecosystems [30–33] and understand the directions and rates of environmental degradation and new soil formation [27,28,34,35].

The aim of the present study was to evaluate partitioning of the chemical elements in surface waters, soils, and plants within the sites affected by abandoned spoil heaps in the Moscow Brown Coal Basin under semihumid climate conditions. We verified the following hypothesis: as the impact of acid mine drainage waters on surrounding ecosystems decreases, concentration of pollutants in soils and plants should decrease.

2. Materials and Methods

The MBCB coal bearing strata mostly belong to the Bobrik, Tula, Aleksin, Mikhailovo, and Venyov suites of the Visean Age (the Middle Mississippian or the Lower Carboniferous subperiod) and are rich in sulfide minerals, e.g., pyrite and marcasite. The basin's bedrock is overlain by calcareous moraines and loess-like loams of the Late Quaternary.

Topographically, the study area (the Kireevsk District of the Tula Region) located within the Moscow Brown Coal Basin on the Central Russian Upland (Figure 1) is characterized as an erosional-denudational weekly plain, dissected by river valleys and a gully network, and has been considerably disturbed by human activities [26]. The valleys are well developed, with wide floodplains and two to three terraces. The exploitation of brown coal shafts has resulted in the formation of man-made landforms such as spoil heaps, tailings ponds, and surface subsidence features [26]. In some mining areas the natural topography has been completely transformed.

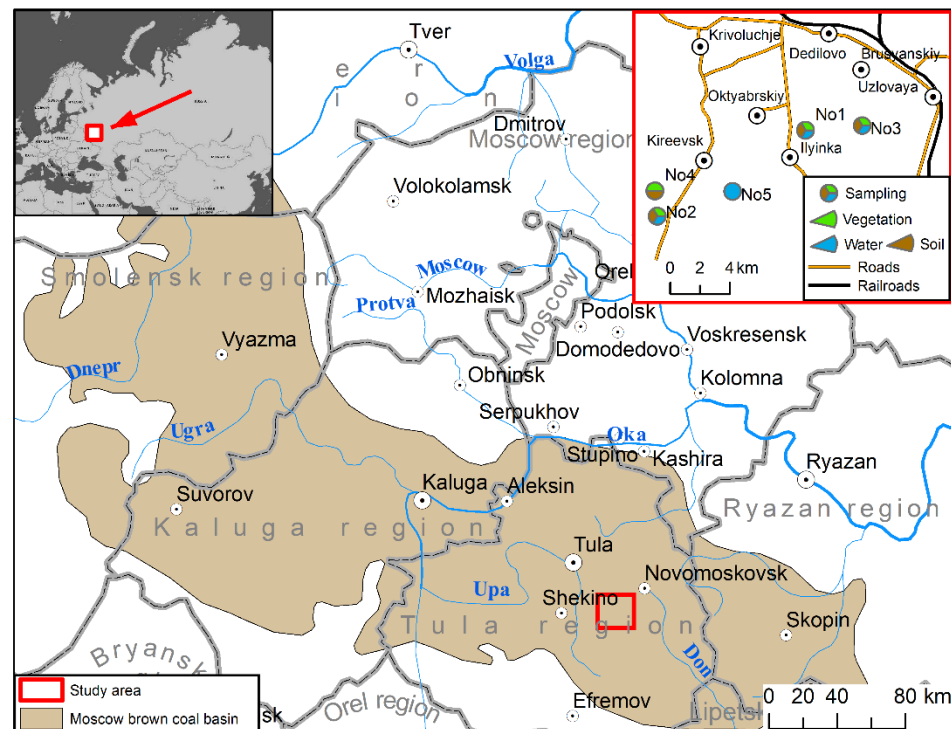


Figure 1. Study area and sites (top right corner) location. Spoil heaps: 1—non-remediated conical, 2—levelled, 3—phytoremediated. 4—unpolluted soil and plant sampling site. 5—unpolluted water sampling site.

According to the Köppen–Geiger Climate Classification, the study area has a snow fully humid climate with a warm summer [36]. The study area is located within the forest-steppe, where woodlands are combined with meadow-steppe communities. Due to farming, native (mostly woodland) communities are preserved in only small areas that are unsuitable for agriculture. The native broad-leaved forests are dominated by *Fraxinus excelsior* and/or *Tilia cordata* and have a thick understory and shrub layer. Their herb layer consists of nemoral species. Occasionally, it is suppressed by strong shade during the summer. Secondary forests are usually dominated by birch (*Betula pendula*) and/or aspen (*Populus tremula*). They have a thin understory of heliophile species such as *Rubus idaeus* and the herb layer is developed with plenty of light, and frequently contains meadow and forest-meadow species. Herb layers of the woodland communities at the bottom of wide U-shaped gullies are usually represented by hygrophyte and nitrophilic mesophyte species. The forest floor in both groups of forests is free of mosses and lichens [28]. Infrequently occurring abandoned arable lands are colonized by meadow communities dominated by (xero-)mesophytes. Another group of meadow communities with a predominance of (meso-)hygrophytes occurs at the bottom of wide gullies. The meadows are often used for moderate-intensity grazing or hay making [37,38].

The black soils—Chernozems (Loamic) and Phaeozems (Loamic)—are found mostly within interfluvial areas of the study area, while Fluvisols are mostly found within river valleys.

Technosols (Spolic) and Regosols develop on spoil heaps within abandoned mine sites. Detailed information on soils of the region under consideration is discussed in [39] and represented in Table S1. Soils and soil horizons are named according to [40,41].

Field work was conducted within three study sites on spoil heaps and two sites in unpolluted territory in August 2020 (see Figure 1 and Table 1). Site 1, at a distance of 2 km to the northeast of the Il'inka village, comprised a non-remediated conical spoil heap 25 m high and 240 m wide at the base. Its steep (about 30°) slopes were dissected by deep (<3 m) gullies. The toeslope colluvial mantle extended to a distance of about 60 m around the perimeter of the spoil heap.

Table 1. Descriptions of the study sites.

Study Site	Topography	Vegetation (Dominants)	Soils
1	Summit and slopes	Single specimens of arboreal species (<i>Betula pendula</i> , <i>Salix caprea</i> , <i>Acer platanoides</i>)	Spolic Technosols (Arenic/Loamic, Dystric, Sulfidic, Phytotoxic) and Technosols (Loamic, Ochric)
		Bare ground	Dystric Colluvic Stagnic Regosols (Arenic/Loamic, Lamellic, Areninovic, Sulfidic, Phytotoxic)
	Talus	Wet meadows (<i>Calamagrostis epigeios</i>) Birch forests with a bare floor or an herb layer, either monodominant (<i>Calamagrostis epigeios</i>) or more rarely poly-dominant	Colluvic Brunic Stagnic Folic Regosols (Arenic/Loamic, Lamellic, Areninovic, Toxic) over Phaeozems (Loamic)
2		Bare ground	Spolic Technosols (Arenic/Loamic, Dystric, Sulfidic, Phytotoxic) and Technosols (Loamic, Ochric)
	Summit	Wet meadows (<i>Calamagrostis epigeios</i>), mixed grasslands (<i>Poa angustifolia</i> , <i>Trifolium hybridum</i> , <i>Lotus corniculatus</i>), and young sparse birch forests with a poly-dominant herb layer	Reductic Spolic Technosols (Arenic/Loamic, Dystric)
	Slopes	Bare ground	Spolic Technosols (Arenic/Loamic, Dystric, Sulfidic, Phytotoxic) and Technosols (Loamic, Ochric)
	Talus	Bare ground	Dystric Colluvic Stagnic Regosols (Arenic/Loamic, Lamellic, Areninovic, Sulfidic, Phytotoxic)
3	Summit and slopes	Mixed grassland dominated by ruderal species (<i>Calamagrostis epigeios</i> , <i>Solidago canadensis</i>)	Technosols (Drainic, Eutric, Folic, Loamic, Molic, Transportic)
		Bare ground	Dystric Colluvic Stagnic Regosols (Arenic/Loamic, Lamellic, Areninovic, Sulfidic, Phytotoxic)
	Talus	Birch forests with a bare floor or a monodominant (<i>Calamagrostis epigeios</i>) or more rarely a poly-dominant herb layer	Colluvic Brunic Stagnic Folic Regosols (Arenic/Loamic, Lamellic, Areninovic, Toxic) over Phaeozems (Loamic)
Unpolluted area	Interfluvial surface	Mixed grassland (<i>Fragaria viridis</i> , <i>Galium mollugo</i> , <i>Tanacetum vulgare</i>)	Calcic Chernozems (Aric, Loamic)
	Gully bottom	Meadow (<i>Alopecurus pratensis</i> , <i>Phleum pratense</i>)	

Site 2, at a distance of 2 km to the southwest of Kireevsk, represented a leveled spoil heap 30 m high and 110 m wide with shortened toeslope colluvial mantle due to the proximity of a U-shaped gully.

Site 3, at a distance of 300 m to the southwest of the Sinyaevka village, represented a levelled spoil heap that was revegetated in 2015. It was 30 m high and 110 m wide at the base, with a 30-m-long toeslope colluvial mantle. Nearby, there were two tailing ponds for

acid mine drainage collection in order to minimize the leakage of acid sulfate waters into the rivers.

Unpolluted territory (Site 4: unpolluted soils) was sampled at a distance of 700–1000 m to the north of Site 2 (on a flat interfluvium and in a gully) and between Site 1 and Site 2 (Site 5: unpolluted pond).

Soil samples (a total of 98, Table S2) 400–500 g each were taken from the A, B, and C horizons and waste rocks in 15 different locations. The samples were dried at 40 °C and crushed with a mortar and pestle to the size of <2 mm, along with the removal of roots and stones.

Plant samples (a total of 22) in the form of birch (*Betula pendula*) leaves and branches of the current growing season were taken in the same locations as soil samples in those cases, where vegetation was present. Birch is the only tree plant that is able to grow in all the areas studied (spoil heaps, talus, and unpolluted territories). The phytomass of herbs and grasses is insufficient to collect appropriate volume of a material for chemical analysis. Air-dried birch samples 100–500 g each were thoroughly cleaned from fragments of any other plant species, dried at 40 °C to reach a constant weight, and ground using a PM-120M rotary grinder (Russia) down to a particle size of less than 1 mm. The ash content in plant samples was determined gravimetrically from the loss on ignition (550 °C) upon reaching a constant weight.

Water samples (a total of 42) were taken from the following groups of locations: surface puddles or ephemeral streams on the spoil heaps (sites 1 and 2) and talus (sites 1, 2 and 3), two tailing ponds (site 3), and the unpolluted pond (site 5). The samples of 1 dm³ in volume were collected in plastic bottles on 12 December 2019, 16 June 2020, 16 July 2020, 22 August 2020, and 12 November 2020 (Table S3). The water samples were passed through paper filters (blue ribbon). Then, pH, electrical conductivity, and the cation and anion compositions were determined in the filtrates.

Soil, plant, and water samples were analyzed using standardized techniques (Table 2). Soil analyses included measurements of total organic carbon, content of chemical elements (including Al, Ca, Co, Cu, Fe, P, K, Mg, Mn, Na, Ni, Pb, and Zn), particle-size distribution (clay < 2 µm; silt 2–63 µm; sand 63–2000 µm), pH (1:2.5 soil-to-water ratio), electrical conductivity (EC), and cation and anion composition (1:5 soil-to-water ratio). The total content of chemical elements was determined using an Axios X-ray fluorescence spectrometer (PANalytical, Almelo, The Netherlands) and Russian Soil Standard samples ('Chernozem' and 'Albeluvisol'), with analytical parameters and standard errors of determination specified in Table S4.

Table 2. Methods of chemical analyses of water, soil, and plant samples.

Parameters	Methods and Equipment
Total organic carbon	The titrimetric method with phenylanthranilic acid [42]
pH	pH-meter 'Expert-pH' (Econix-Expert Ltd., Moscow, Russia), soil: solution ratio 1:2.5
Grain-size fractions	A laser diffraction technique and Analysette 22 equipment (Fritsch, Idar-Oberstein, Germany) in samples pre-treated with 4% Na ₄ P ₂ O ₇
Total content of elements in soil samples	Axios X-ray fluorescence spectrometry (PANalytical, Almelo, Netherlands); a powder (<0.067 mm)
Total content of elements in plant samples	Acid digestion (concentrated HNO ₃ and H ₂ O ₂). Elan-6100 inductively coupled plasma mass spectrometer and an Optima-4300 DV inductively coupled plasma atomic emission spectrometer (PerkinElmer Inc., Waltham, Massachusetts, United States)
Electrical conductivity	Hanna HI 98331 (Woonsocket, Rhode Island, United States), soil-to-water ratio 1:5

Table 2. Cont.

Parameters	Methods and Equipment
Cation and anion composition (Cl^- , NO_3^- , SO_4^{2-} , Ca^{2+} , Mg^{2+} , Na^+)	A 'Styer' liquid chromatograph with an amperometric detector (Aquilon, Saint Petersburg, Russia)
Anions HCO_3^- and CO_3^{2-}	Acid-base titration using a 0.01 M H_2SO_4 solution
Mobile fractions:	Parallel extraction; incubation for 18 h [43–45]; AES-ICP detection (iCAP-6500, Thermo Scientific, Waltham, MA, USA):
F1	NH_4Ac (ammonium acetate buffer); soil-to-water ratio 1:5; pH 4.8
F2	NH_4Ac with 1% EDTA (ethylenediaminetetraacetic acid); soil-to-water ratio 1:5; pH 4.5
F3	1 M HNO_3 (nitric acid); soil-to-water ratio 1:10; pH 0.0

The chemical element extractability was analyzed using a parallel extraction procedure. Mobile fractions of chemical elements were extracted from soil samples using NH_4Ac (Fraction F1), NH_4Ac with 1% ethylenediaminetetraacetic acid (EDTA) (fractions F1 + F2), and 1 M nitric acid (fractions F1 + F3). The analyzed fractions named as in [43] are defined as follows [43,44]:

- F1 (exchangeable): weakly bound acid-soluble (water-soluble and bounded with carbonates and exchangeable ions).
- F2 (complex): bound with complexes (predominantly, fulvate and humate substances).
- F3 (specifically adsorbed): bound with different soil phases (Fe and Mn (hydr)oxides, with carbonates, with sulfides, and with some clay minerals) [46–49]. The solution of 1 M nitric acid simulates the conditions generated by oxidation at the surface of sulfide minerals [50].
- F4 (residual): residual mineral fraction calculated as a difference between the total content of the chemical elements and the concentration of the mobile fractions F1 + F2 + F3.

The concentration of the chemical elements in the extracts and water was determined using an iCAP-6500 inductively coupled plasma atomic emission spectrometer (Thermo Scientific, Waltham, MA, USA) and blank solutions of NH_4Ac , NH_4Ac +1% EDTA, and 1M HNO_3 . Duplicate measurements were made in 5% of the samples (Table S5) for analytical quality validation.

In the plant samples after acid digestion (Table 2), the total content of Al, Ca, Co, Cu, Fe, K, Mg, Mn, Na, Ni, P, Pb, S, and Zn was measured by inductively coupled plasma mass spectrometry and inductively coupled plasma atomic emission spectrometer. Along with the analyzed samples, the control samples of birch leaves (COOMET CRM 0067-2008-RU, Irkutsk, Russia) [51] and tobacco leaves (INCT-OBTL-5) [52] were digested for quality control (Table S6). Duplicate measurements were made in 20% of the samples for analytical quality validation.

Data processing included the calculation of the chemical element (ChE) extractability (E):

$$E = \frac{F1 + F2 + F3}{TC} \times 100 \quad (1)$$

where F1, F2, and F3 are the concentrations of chemical elements in the mobile fractions (mg/kg) and TC is the total content of a ChE. To assess main trends in partitioning of the studied ChEs, we calculated geochemical indices L, Kx, PWR, Ax, and Bx. The L-index is the average content of a chemical element in a soil horizon normalized to the average content of the same ChE in the corresponding horizon of Technosols or unpolluted Chernozems [53]. The L-index values below 0.8 and above 1.3 characterize the zones of leaching and accumulation, respectively [54]. We calculated L-indices for ChEs in waters and plants from the coal mining sites as compared to the unpolluted territories. Kx, which

reflects the relationship between the chemical composition of rocks (soils) and surface waters was calculated using the following equation:

$$K_x = \frac{100 \times m_x}{M \times C_x} \quad (2)$$

where m_x —concentration of the chemical element in water (mg/dm^3), C_x —concentration of the ChE in rock (%), and M —mineralization of water (g/dm^3) [55]. All ChEs were merged into four groups depending on K_x values as follows: very highly mobile ($K_x > 10$), highly mobile (1–10), mobile (0.1–1.0), and slightly mobile or inert (<0.1). The plant–water ratio (PWR) is a ratio of ChE concentration in plant ash to its concentration in surface waters [56]. The A_x and B_x indices characterize the intensity of absorption of chemical elements by plants, with A_x being the ratio of ChE concentration in plant ash to its average concentration within the topsoil (0–20 cm layer) [21,55] and B_x being the ratio of ChE concentration in dry plant material to the concentration of its F1 fraction within the topsoil [57].

Differences in the concentration of chemical elements were determined for paired datasets using the Mann–Whitney U test. Spearman correlation analysis was conducted to identify relationships between chemical elements and environmental conditions.

In this paper, we focused on HMMs, including potentially toxic elements such as Ni and Pb, and considered Ca, Fe, and S as typomorphic elements [21,53,54], and Co, Cu, K, Mg, Mn, Na, P, and Zn as biologically active elements [58]. Moreover, we chose Co, Cu, Fe, Mg, Mn, Ni, P, Pb, S, and Zn as elements whose content is monitored in surface waters and/or soils of Russia [59–62].

3. Results and Discussion

In the Moscow Brown Coal Basin, abandoned coal spoil heaps were found to be associated with toeslope talus mantle and contamination of surface waters and soils with potentially toxic elements due to the evolution of the acid sulfate soils. This fact should be taken into account in the life cycle assessment of brown coal mining, which is rich in sulfide minerals. Our study was conducted to uncover the impact of acid mine drainage on the ecosystems of the toeslope talus mantle and the formation of new ecosystems.

3.1. Geochemical Partitioning of Elements in Surface Waters

Water from the unpolluted pond had a neutral reaction ($\text{pH } 7.1 \pm 0.6$) and a low content of electrolytes ($\text{EC } 46 \pm 19 \text{ mS}/\text{m}$). Surface water samples from the spoil heaps were significantly more acidic ($\text{pH } 3.7 \pm 0.3$, $p = 0.0012$) due to the high content of sulfates ($2.9 \pm 1.4 \text{ g}/\text{dm}^3$, $p = 0.0012$). This induced the mobilization (dissolution) of many HMMs [63]. Water samples from the talus had higher pH values and lower content of sulfates and HMMs (Table S7). However, their levels were significantly different from the levels in the unpolluted pond. Water samples from the two tailing ponds were relatively closer in composition to the unpolluted waters. The concentration of potentially toxic elements (e.g., Fe) in the tailing pond located farther from the mine was similar to that in the unpolluted pond, but the electrical conductivity and the concentration of sulfates, K, Mg, Ca, Mn, Co, Ni, and Zn was still higher than the background levels (Figure 2).

The L-index values showed that positive anomalies of the analyzed parameters were more prominent than negative anomalies (Table S8), which reflected the saturation of acid-sulfate waters with different chemical elements including potentially toxic elements (Al, Co, Cu, Fe, Mn, Ni, Pb, and Zn).

Therefore, the highly saline acid mine drainage enriched in potentially toxic elements had affected all studied mine site ecosystems.

3.2. Geochemical Partitioning of Elements in Soils

3.2.1. Physico-Chemical Properties

The unpolluted Chernozems (Loamic) were characterized by a nearly neutral pH, a low electrical conductivity, a high total organic carbon content decreasing with depth, a

prevalence of the fine silt, and the absence of sand fractions (Figure 3, Table S9). Such characteristics are typical for Chernozems within the Central Russian Upland [64–68].

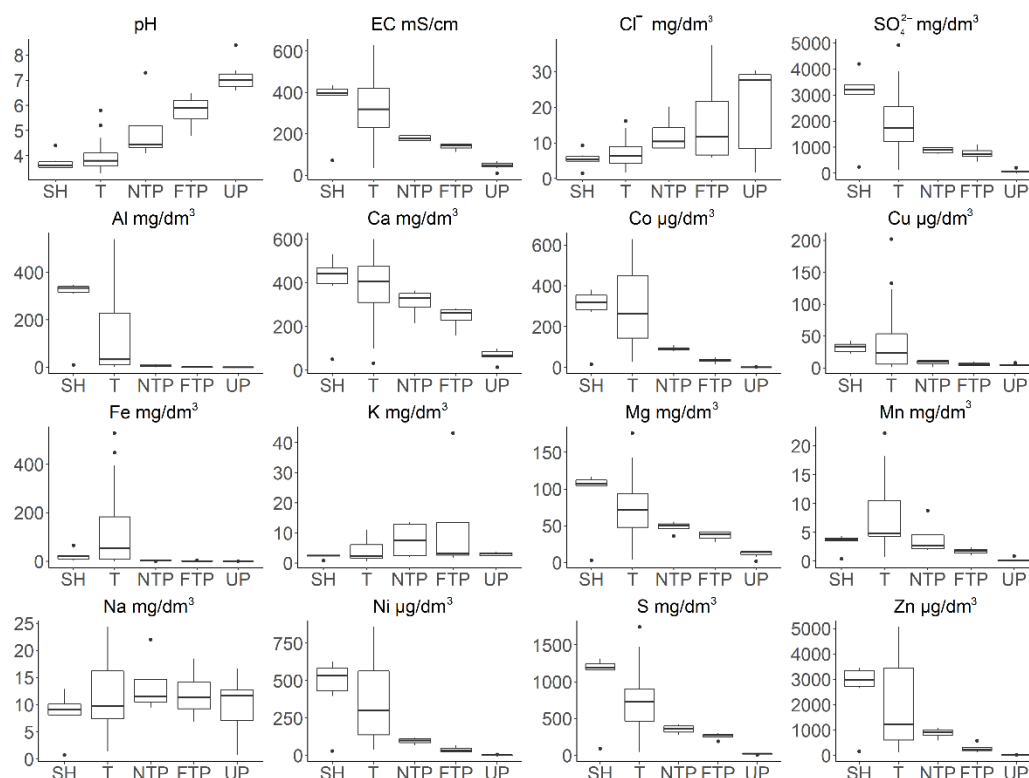


Figure 2. Variation of pH, electrical conductivity, and the concentration of anions and chemical elements in surface water sampled in 2019–2020 in the surface Moscow Brown Coal Basin. SH—spoil heaps, T—talus, NTP—nearer tailing pond, FTP—farther tailing pond, UP—unpolluted area. Bold line is the median. Box borders represent the inter quartile range (IQR) between the first (Q1) and the third (Q3) quartiles. Whiskers are $Q1 - 1.5 \times IQR$ and $Q3 + 1.5 \times IQR$ intervals. Outliers are shown as separate points.

The Spolic Technosols on the spoil heaps had highly variable pH, electrical conductivity, total organic carbon, and sand contents due to the initial heterogeneity of the waste rocks [39]. As compared to the unpolluted Chernozems, the studied Technosols had a significantly higher content of sand ($63\text{--}2000\ \mu\text{m}$, $p < 0.016$), but a lower content of fine silt ($2\text{--}20\ \mu\text{m}$, $p < 0.001$), and also a higher electrical conductivity ($p < 0.001$) and a lower pH ($p = 0.046$).

Under the influence of acid mine drainage, buried Chernozems lost carbonates. Therefore, we named buried soils as phaeozems. However, their development under conditions of high moisture may lead to their transformation into Gleysols, since stagnic color patterns were observed in subsoils during the field studies. Revealing the rate and reversibility of such changes can be a special research topic [69].

In the Moscow Brown Coal Basin, Technosols differed in the composition of the soil matrix from the surrounding Chernozems, making differences in texture and elemental composition reliable diagnostic criteria to assess the degree of transformation of affected soils, which can be used to classify buried soils or soils exposed to any chemical attack. Similar ideas were explored in [70].

Changes in soil properties reflects the most serious and long-lasting effects of the environment [71–74] due to the buffer properties. Due to pedogenesis, the accumulation of some substances resulted in the formation of geochemical barriers in soil compartments [23–25]; organic matter provides formation of a biogeochemical barrier, clay minerals and Fe and Mn hydroxides, a sorption barrier, carbonates, a carbonate barrier, etc. Over time, the buffering

capacity of the soil may be exceeded. Therefore, exposure time should be considered in the context of the influence of acid mine drainage on ecosystems. The Kizel Brown Coal Basin studies [18] demonstrated that in the first stages of geochemical transformation of soils within the zones affected by acid mine drainage, HMMs accumulate in the toeslope colluvial mantle. Leaching of HMMs from waste-rock dumps and topsoils of Technosols begins about 50 years from the onset of pollution and results in the formation of negative anomalies in the dumps and positive anomalies in the surrounding soils [18,75]. We observed similar trends in the key area studied. In a spontaneously vegetated urban brownfield located in New Jersey, downward migration of heavy metals and metalloids from the Technosol topsoils (a 0–5 cm layer) and subsequent immobilization in the subsoil (a 5–25 cm layer) were observed in 50 years since site abandonment [76]. Long-term exposure of Andosols to steam-heated acid-sulfate waters resulted in the formation of endothermal soils [77–79] or Narcisols [15], which differed in texture, elemental, and mineralogical composition from surrounding non-affected soils.

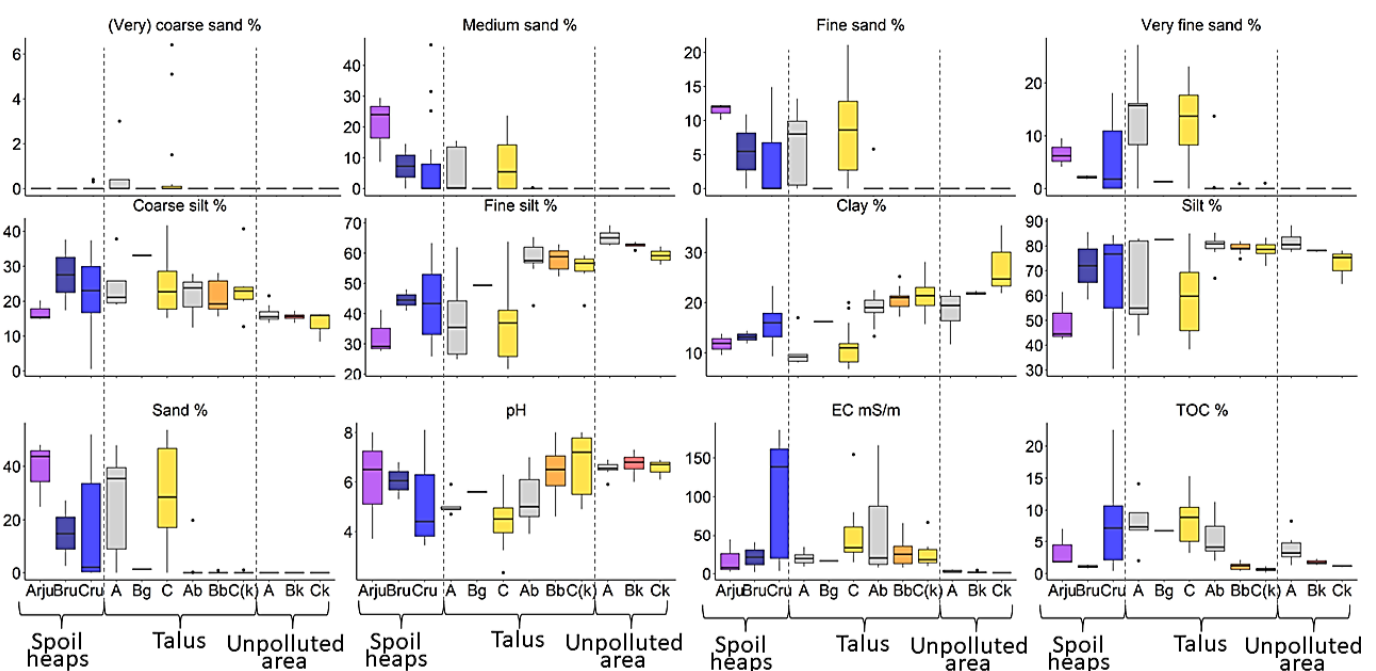


Figure 3. Variation of the physico-chemical properties of the soil horizons sampled in 2020 in the surface Moscow Brown Coal Basin. Bold line is the median. Box borders represent the inter quartile range (IQR) between the first (Q1) and the third (Q3) quartiles. Whiskers are $Q1 - 1.5 \times IQR$ and $Q3 + 1.5 \times IQR$ intervals. Outliers are shown as separate points.

3.2.2. Special Differentiation

The Regosols formed on the toeslope colluvial mantle represented a transitory medium with a predominant accumulation of the studied HMMs (Figure 4). These soils were characterized by increased content of at least two mobile fractions of Al, Co, Fe, K, Mn, Na, Ni, P, and Zn, but decreased content of mobile fractions of Ca, Mg, and Pb (Table S10). In a former mining area in NW Tunisia (with the exploitation of Pb-Zn and Fe ore deposits between 1881 and 1958), the total concentration of heavy metals decreased abruptly with distance from the flotation tailings and mining facilities [80].

Under the talus mantle, the Ab-horizon of Chernozems was transformed into a leaching zone with $L < 0.8$ in 52% of the studied chemical elements, and the Bb and C horizons were transformed into accumulative zones, with $L > 1.3$ in 59 and 72% of ChEs, respectively. According to [81], we observed a downward-translocation-solutional catena. Indeed, the soils buried and formed at the footslope of the spoil heaps can be considered as geochemical barriers on the migration route of potentially toxic elements.

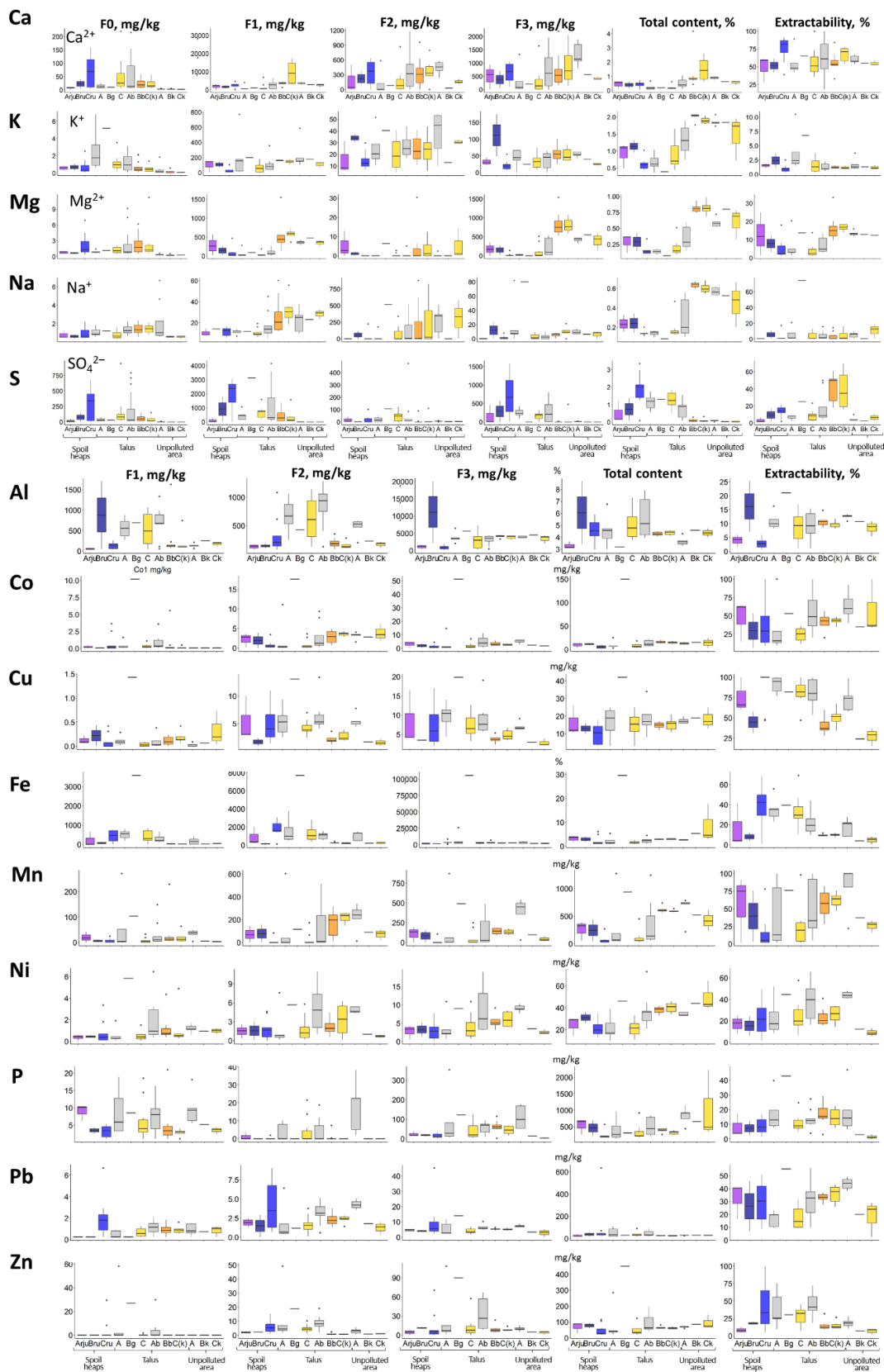


Figure 4. Variation of the elemental composition of the soil horizons sampled in 2020 in the Technosols of the Moscow Brown Coal Basin. Bold line is the median. Box borders represent the inter quartile range (IQR) between the first (Q1) and the third (Q3) quartiles. Whiskers are $Q1 - 1.5 \times IQR$ and $Q3 + 1.5 \times IQR$ intervals. Outliers are shown as separate points.

Spatial differentiation in the total concentration of chemical elements (based on L-indices) was lower than those in any of mobile fractions of the same ChE. This had previously been reported from catenary studies on unpolluted soils of the Central Russian Upland [65,82]. Based on L-indices in all studied soil horizons, the differences between the positive anomalies of the analyzed parameters were greater than between the negative anomalies (Table S10). This reflects a predominance of the accumulation over the depletion of substances within the talus material.

3.2.3. Extractability

In the studied Technosols, Regosols, and Chernozems, the content of different fractions of chemical elements had the same decreasing orders (Figure S1). In the soils studied, the extractability of chemical elements decreased in the following order: Ca > Cu > Mn, Co, Pb, Zn > Ni, Fe, P, Al, S, Mg > Na, K (Figure 5). According to this order, several groups of chemical elements were distinguished depending on their extractability. Alkaline major elements (K and Na) in most cases had a (*very*) *low extractability* ($E < 10\%$), except for some soluble compounds of Na that were either derived from acid mine drainage or formed in the C horizons of Chernozems. Most complex-forming cationic (Mg, Al, Fe, Ni) and anionic (S and P) elements had a *low extractability* ($E = 5\text{--}20\%$). Another group included Co, Mn, Pb and Zn, which were generally characterized by *moderate extractability* ($E < 50\%$ in the most of the studied soil horizons, see Table S9), except for some cases when their extractability values increased within the impact zones of acid mine drainage.

Soils	Horizons	K	Na	Mg	S	Al	P	Fe	Ni	Zn	Pb	Co	Mn	Cu	Ca
Technosols	Arju, n=3	2	1	12	2	4	4	4	18	8	41	62	75	66	59
	Bru, n=2	2	6	8	9	16	7	8	15	18	26	29	39	44	52
	Cru, n=15	1	1	2	14	3	8	42	21	33	30	29	5	100	82
Regosols	Arju, n=1	2	1	2	9	9	8	36	8	10	20	10	2	100	46
	Cru, n=9	1	1	2	8	6	9	41	17	16	24	16	13	83	53
	2Ayg, n=3	1	16	4	19	1	14	44	40	72	56	45	23	100	83
	2Bgb, n=4	1	6	14	40	11	15	9	25	11	31	39	42	34	55
	2Cg, n=1	1	9	16	24	10	21	9	14	11	29	35	47	34	54
Regosols over Phaeozems	Ag, n=4	3	4	4	7	11	16	32	23	40	15	23	47	89	51
	Bg, n=1	7	74	14	25	21	43	39	45	30	55	53	76	82	65
	Cg, n=6	2	4	4	8	12	11	27	24	35	10	31	22	81	51
	2Ayb, n=18	1	2	6	8	11	12	19	42	40	29	57	38	77	58
	2Bb, n=11	1	0	15	50	10	17	9	19	14	34	43	65	40	53
	2Ck, n=5	1	1	18	46	10	10	10	32	13	40	45	66	52	74
Chernozems	A, n=8	1	6	13	4	13	14	21	44	18	44	60	100	74	58
	Bk, n=1	1	1	13	2	11	3	4	12	7	20	35	37	24	55
	Ck, n=3	1	13	12	6	9	1	5	8	9	24	37	28	29	53

Figure 5. Chemical element partitioning in the soils studied. The chemical element extractability (median) is indicated by colors: red <5%, orange 5–10%, yellow 10–50%, and blue >50%. Soil horizons are named according to [41]: A—mineral surface horizons, B—subsoil horizons, C—parent materials; b—buried, g—stagnic conditions, j—jarosite accumulation, k—accumulation of pedogenetic carbonates, r—strong reduction, u—urban and other human-made materials, y—pedogenetic accumulation of gypsum.

An analysis of chemical speciation indicated that Al, K, Mg, and Na were mainly in residual fractions, which made up more than 80% of their total content, while the percentage of each mobile fraction was below 15%. In most of the studied soil horizons, the residual fraction of Fe, Ni, P, Pb, S, and Zn had content of under 50%, while the percentage of each

mobile fraction was below 15%. Calcium was mainly in the exchangeable fraction, which made up 30% of its total content. The percentage of exchangeable Al, Cu, Fe, K, Ni, P, and Pb was low (<5%). Specifically adsorbed compounds always prevailed over F2 in Ca, Cu, Fe, Ni, P, Pb, and Zn. Na was characterized by a reverse situation. In some horizons of the native or post arable Chernozems (including buried soils), the content of complexed compounds of biologically active Co, Mn, S, and Zn was higher than the content of their specifically adsorbed compounds.

Despite the material of spoil heaps and talus material being rich in potentially toxic elements and differing considerably in physico-chemical properties, the proportion of mobile compounds in the total content of chemical elements in the A-horizons are constant (Figure S1). Previously, similar geochemical partitioning (insignificant differences between sharply diverse soils) was reported for Kastanozems and Solonetz at the Ergeni Upland [83], in Podzols affected by acid mine drainage on a hillslope in Dalarna, soils of central Sweden [84] and soils at a different distance from the basements of spoil heaps were rich sulfur compounds [85]. That is, the ratio of different compounds of the same chemical element weakly depends on the properties of the soil and is more determined by the chemical properties of the element and the geochemical specialization of the parent material. For example, the extractability of Ca, Co, and Mn is high in the A-horizons of the acid Spolic Technosols and the acid-free Chernozems, but extractability of Al, S, and K is low. Similarities in the orders of mobility of ChEs in topsoils and in terms of geochemical spectra of ChEs that accumulate and disperse within soils was originally observed in Retisols, Phaeozems, and Chernozems within the Volga Upland of the East European Plain [86], and in the topsoils of Chernozems and Planosols in the Trans Urals [45].

In addition, biologically active Co and Mn had increased E values within the A horizon of unpolluted soils, which has been mentioned before in the studies on Chernozems of the Central Russian Upland [64,65,82] and Trans-Urals [45,87,88]. Mobile fractions of those chemical elements have also been found in young soils at the top of spoil heaps and on the toeslope colluvial mantle [89]. Cu was characterized by a *high extractability* and Ca—by a *very high extractability*, i.e., $E > 45\%$ in all studied soil horizons, which confirmed our previous findings [83,90].

3.3. Geochemical Partitioning of Elements in Plants

Ash content in birch leaves was higher than that in birch branches (Figure 6), without any significant differences between plants growing on the spoil heaps, talus, and in the unpolluted area. Concentrations of chemical elements in the aerial tissues of birch decreased in the following order: K, Ca > Mg, S, P > Mn, Fe, Zn, Al > Na > Cu, Ni, Co, Pb. The leaves had relatively higher contents of Al, Ca, Fe, K, Mg, Ni, P, and S (Table S11). Trees growing on the spoil heaps and the talus had very few differences in chemical composition, including higher ($p = 0.017$) content of Ni in both leaves and branches sampled from the talus and Pb in the leaves from the birches on the spoil heaps, as well as tendencies ($p = 0.087$) for higher concentration of K in both leaves and branches of birches on the spoil heaps. Higher concentration of Ni and Pb may have resulted from their passive absorption by plants [91] growing at the contaminated soils. From the spoil heaps to their talus and further to the unpolluted area, there were increasing concentration of Co, K, and Mn, which are essential to plants [58]. and decreasing concentration of Ca and Pb in birch leaves and branches. Content of other chemical elements (Al, Cu, Fe, Mg, Na, Ni, P, S, and Zn) in birch aerial tissues did not show any significant differences between the study sites.

Birch leaf enrichment in Al, Ca, Fe, K, Mg, Ni, P, and S compared with branches resulted from biogeochemical partitioning in aerial plant tissues, as all these elements excluding Al are essential for plants and participate in different biochemical processes [58].

In birch, the positive and negative anomalies of concentrations of the studied ChEs were similar to the L-indices in terms of differences between the values (Table S12). The assemblages of accumulated and dissipated chemical elements were also similar. All these findings reflected the plant's capability to maintain certain ranges of element concentrations

in their tissues. Previously, a relatively low ability of phytoextraction of heavy metals by birch from contaminated soils was reported in [92].

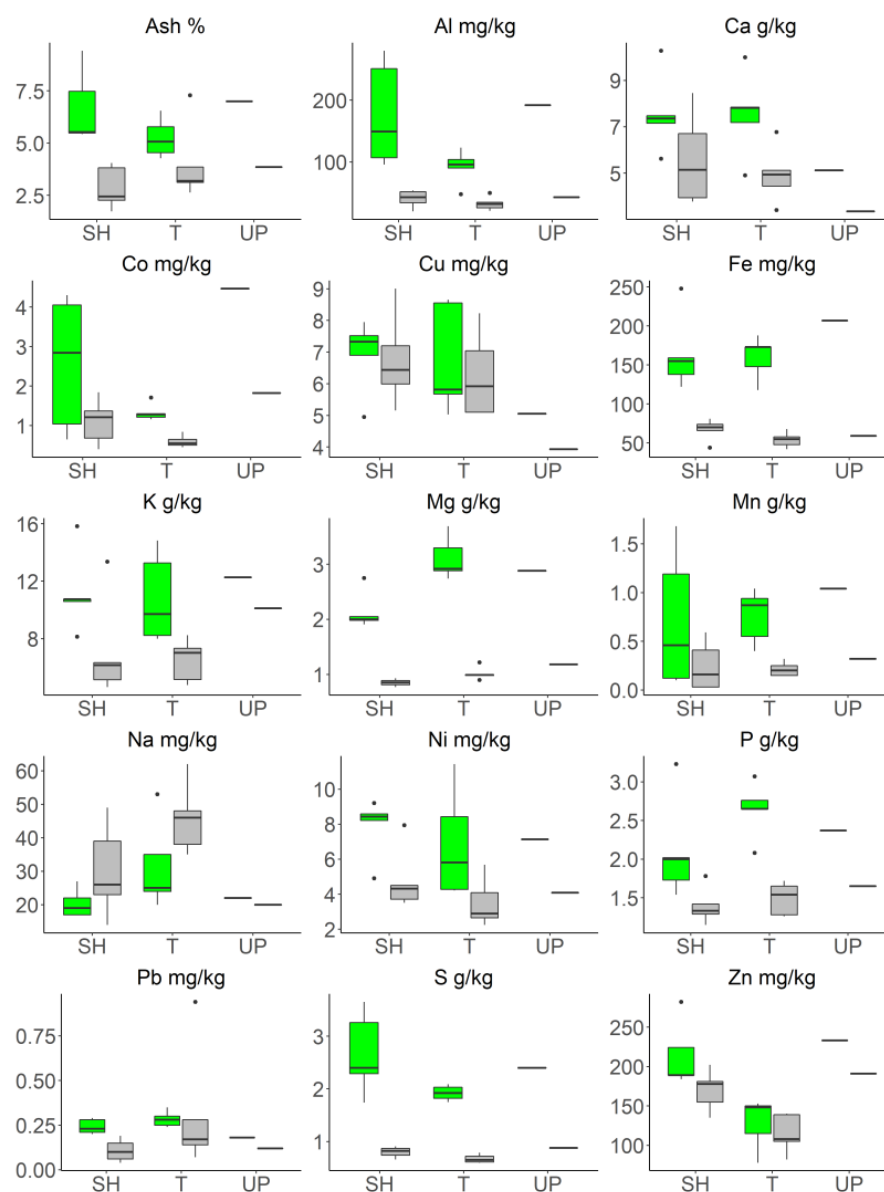


Figure 6. Variation of the ash content and the elemental composition of the birch aerial tissues (green—leaves, grey—branches) collected in 2020 in the Moscow Brown Coal Basin: SH—spoil heaps, T—talus, FTP—farther tailing pond, UP—unpolluted area. Box borders represent the inter quartile range (IQR) between the first (Q1) and the third (Q3) quartiles. Whiskers are $Q1 - 1.5 \times IQR$ and $Q3 + 1.5 \times IQR$ intervals. Outliers are shown as separate points.

In accordance with the phylogenetic specialization of certain species [91,93–95], vegetation can also be a very informative indicator of the influence of acid mine drainage. However, when assessing the degree of influence of acid mine drainage, it is necessary to take into account the presence of physiological barriers that prevent the entry of toxic elements into plant tissues. It is necessary to choose species that are sensitive to exposure and passively absorb indicator elements. It should be noted separately that it is important to choose species of broad ecological specialization that can survive in a wide range of pollution in order to compare the background and the most polluted areas. Stability of the chemical composition of plants within the impact zones of acid mine drainage was reported before, e.g., at a gold mine site in the northwest of Quebec [96], in the Portuguese

sector of the Iberian Pyrite Belt [97], and in semi-arid northeast Brazil [98]. Similar levels of Al, Ca, Mg, and Mn were found in the aerial tissues of *Betula nigra* (L.) grown on the soils influenced by acid mine drainage in SW Ohio [99], as well. A relatively higher content of chemical elements in birch leaves compared with birch branches was found in [99].

3.4. Relationships between the Chemical Composition of Surface Waters, Soils, and Plants

Based on the results obtained, we can conclude that to assess the degree of influence of acid mine drainage on changes in ecosystems, first of all, water should be sampled as a main indicative media. It is likely that we could obtain more contrasting patterns by analyzing soil waters or drying up ponds, rather than temporary streams. We think that the water of sampled temporary streams changed weaklier due to shorter contact with the solid phase of soils. Analysis of the elemental composition of plants in our case gave the most blurred picture. However, using more sensitive plant species with less phytomass in similar areas or species that are less susceptible to acid mine drainage may provide more interesting results.

In the studied locations, difference between the chemical composition of the sampling medium decreased in the following order: surface waters > soils > plants (Figure 7). This could be explained by the presence of geochemical barriers in soils and physiological barriers in plants. It had been shown that both terrestrial and aquatic plants have low levels of accumulation of chemical elements within impact zones of acid mine drainage waters, e.g., in the Iberian Pyrite Belt (Portugal), the north Morocco mining areas [100], the São Domingos mine site, the southeast of Portugal, Alentejo Region [101], and the Dabaoshan Pyrite/Copper Mine, Guangdong Province, China [89]. However, the composition of soils and waters within such zones significantly differed from those in unpolluted area.

Proxy	Surface waters				Soils												Plants (birch)							
					Bulk sample				F1				F2				F3				Leaves		Branches	
	Arju		2Ayg		Arju		2Ayg		Arju		2Ayg		Arju		2Ayg		I	II	I	II				
	I	II	IIIa	IIIb	IIa	IIb	IIa	IIb	IIa	IIb	IIa	IIb	IIa	IIb	IIa	IIb								
pH	0.5	0.6	0.7	0.8	0.8	0.8	0.8	0.8	not determined				not determined				not determined							
EC	7.0	6.4	3.6	2.8	1.4	1.1	20.5	14.0	not determined				not determined				not determined							
Al	1395	675.0	32.0	2.0	0.9	1.5	1.2	1.5	6.2	10.2	0.5	6.0	1.9	6.0	0.3	1.9	1.9	6.0	0.3	1.9	0.8	0.6	1.1	0.7
Ca	5.8	5.6	4.6	3.6	0.2	0.7	1.0	0.6	0.2	0.8	0.9	0.7	<0.01	1.0	1.5	0.8	<0.01	1.0	1.5	0.8	1.6	1.4	1.7	1.5
Co	347.5	367.5	113.8	42.5	0.3	1.2	0.9	1.0	0.3	2.5	18.4	10.5	0.05	1.4	0.3	1.0	0.05	1.4	0.3	1.0	0.3	0.5	0.3	0.5
Cu	7.4	10.0	1.9	1.3	1.4	1.9	0.6	0.9	0.2	1.2	3.7	2.7	0.5	1.2	0.9	1.2	0.5	1.2	0.9	1.2	1.2	1.4	1.6	1.7
Fe	80.0	393.3	9.7	3.7	0.3	0.8	0.7	1.0	1.6	2.5	1.2	1.8	0.7	2.1	1.5	1.0	0.7	2.1	1.5	1.0	0.8	0.8	1.1	1.0
K	0.8	1.3	2.6	4.4	0.4	0.8	0.7	0.8	0.07	2.8	0.2	0.5	0.7	1.9	0.7	0.7	0.7	1.9	0.7	0.7	0.7	1.0	0.5	0.8
Mg	7.6	6.3	4.0	3.0	0.3	0.5	0.6	0.6	0.05	0.3	0.1	0.3	<0.01	<0.01	<0.01	1.2	<0.01	0.0	<0.01	1.2	1.0	0.9	0.8	0.8
Mn	17.4	37.4	21.6	8.9	0.2	1.5	0.6	0.6	0.05	4.1	0.5	1.0	<0.01	2.3	<0.01	0.6	<0.01	2.3	<0.01	0.6	0.5	0.8	0.4	0.8
Na	0.8	1.2	1.4	1.2	0.7	0.5	0.6	0.6	1.0	1.0	0.5	0.8	<0.01	12.5	0.8	0.4	<0.01	12.5	0.8	0.4	1.1	1.2	1.8	2.0
Ni	215.2	159.5	45.2	18.1	0.4	1.0	0.9	1.1	0.2	1.9	1.0	1.7	0.07	1.7	1.0	1.1	0.07	1.7	1.0	1.1	0.6	1.2	0.7	1.1
P	0.4	0.5	0.5	0.4	0.2	0.9	0.7	0.7	0.4	1.1	0.4	0.8	<0.1	3.8	<0.01	0.3	<0.1	3.8	<0.01	0.3	0.9	1.0	0.8	0.9
Pb	1.4	2.5	1.5	0.5	0.7	2.4	0.7	1.7	1.0	2.2	1.6	1.1	0.2	1.2	0.7	0.7	0.2	1.2	0.7	0.7	1.7	1.3	3.7	1.0
S	54.3	41.5	18.6	13.6	1.6	2.4	10.5	8.9	4.6	4.8	190.6	126.4	0.9	1.4	15.3	12.0	0.9	1.4	15.3	12.0	1.0	0.9	0.8	0.9
Zn	260.9	208.7	88.1	28.7	0.3	1.5	0.9	1.4	na	na	>38	>46	0.9	8.0	3.1	2.9	0.9	8.0	3.1	2.9	0.7	0.7	0.8	0.7

Figure 7. Spatial distribution of chemical elements in surface waters, plants and soils affected by acid mine drainage. Numbers are L-index values (for the Arju and 2Ayg horizons, they are calculated as normalized values for the Arju and A horizons sampled in the spoil heaps and background area, respectively): red >10%, orange 10–2%, yellow 2–1.3%, white 1.3–0.8, blue 0.8–0.5, dark blue 0.5–0.1, very dark blue <0.1. I—spoil heaps, II—talus (a—bare ground, b—meadows and forests), III—tailing ponds (a—nearer, b—farther).

We confirmed that acid mine drainage causes considerable impacts on the elemental composition of surface waters, newly formed soils, and old black soils, but the elemental composition of aerial tissues of birch grown on the toxic materials at the spoil heaps and the toeslope talus and on the non-contaminated loess-like loams differs inconsiderably. Preceding studies on the sustainability aspects of ecosystems located in similar talus mantle

and spoil heaps are sparse [102]. Therefore, the findings presented here cannot be compared with much preceding research. Influx of acid mine drainage to arable lands surrounding studied spoil heaps results in pollution of crops with potentially toxic elements, which is a typical problem in such cases and is previously reported, e.g., in [103,104]. Our findings are in line with the works by N.P. Solntseva [18–20,22,105], who concluded that changes in the elemental composition of affected surface waters and soils depend on the period of self-remediation of the abandoned mining area and are similar in the diverse regions.

Due to the considerable differences in the chemical composition of the studied surface waters, the geochemical indices of Kx and PWR had a wide range of values. This is reflected in the trends of changes in the mine sites compared to the unpolluted sites (Table 3). Only in the case of Na were both Kx and PWR values in the mine sites higher than those in the unpolluted area. This was probably caused, firstly, by a low concentration of Na in acid mine drainage waters and newly formed soils (Technosols and Regosols) developed under semihumid conditions and, secondly, by Na assimilation by plants without any geochemical barriers under conditions of low Na concentration within the root zone.

Table 3. Values of the geochemical indices that characterize the relationship between the chemical composition of surface waters, soils, and plants.

Chemical Elements	Kx			PWR			Ax			Bx		
	Spoil Heaps	Talus	Unpolluted Area									
Na	1.6	0.6	0.5	0.009	0.008	0.004	0.49	0.61	0.07	2.1	3.1	0.8
Mg	17	3.9	0.5	0.036	0.047	0.298	23	26	6.2	108	51	5.5
Al	1.7	0.8	0.002	0.001	0.001	0.819	0.05	0.03	0.05	2.0	0.11	0.9
P	36	27	28	1173	1169	472	136	143	42	278	337	217
S	19	38	7.1	0.003	0.004	0.148	2.2	2.2	32	5.8	3.8	158
K	0.09	0.06	0.04	6.2	5.5	7.4	15	33	12	49	82	74
Ca	20	16	2.3	0.04	0.04	0.12	32	93	9	3.1	10.3	1.1
Mn	16	3.4	0.08	1725	1763	61,162	106	147	16	478	119	18
Fe	0.4	1.2	0.002	0.009	0.002	0.883	0.058	0.140	0.088	0.8	0.2	0.9
Co	10,159	5778	14	0.06	0.11	68	1.9	4.6	4.3	8	6	42
Ni	4817	2415	15	0.17	0.43	50	2.9	6.0	3.2	11	16	5
Cu	686	690	65	5	4	20	13	8	5	70	76	150
Zn	22,240	8605	35	1	2	425	61	81	60	>1500	>1500	>2000
Pb	85	180	72	0.91	0.20	0.35	0.24	0.10	0.10	1.5	0.7	0.2

Values that are 10 times as high and low as the background levels are marked in red and blue, respectively. Differences by 100 times are shown in bold.

The chemical elements were grouped according to their Kx values. Co, Cu, Ni, Zn, P, and Pb were very highly mobile ($Kx > 10$) in all study sites, with the first four metals characterized by $Kx > 100$ due to their extremely high concentration in acid mine drainage waters of the spoil heaps and the talus, according to the Russian drinking water quality standards (Table S13). Potassium was weakly-mobile or inert. At the spoil heaps and the talus, the Kx values of Na, Mg, S, and Ca were dozens of times higher than those in the unpolluted site, whereas Al, Fe, and Mn values were at least 100 times higher. Therefore, Al, Fe, and Mn could be regarded as typomorphic elements within the zones affected by acid mine drainage, but not within the unpolluted areas, because they were incapable of active migration within a near-neutral medium, according to existing geochemical concepts [21,106–108].

In terms of Ax and Bx indices, differences between studied sites were less considerable than the differences in the Kx and PWR indices. This was due to the presence of physiological barriers in plants that prevented the assimilation of harmful levels of potentially toxic elements [58,91]. This trend was most clearly expressed in S, which was one of the most actively assimilated nutrients from unpolluted soils [55,58,109]. Despite the fact that the concentration of bioavailable compounds of S drastically increased in waste rocks, where S was a typomorphic element, the S concentration in birch aerial tissues remained at levels similar to those of the unpolluted area.

There was a positive correlation between the content of all considered chemical elements in leaves and branches of birch. However, the correlation was significant in only half of the studied elements, including Mg, Al, S, K, Ca, Mn, Co, and Ni (Table S14). The chemical composition of plants did not significantly correlate with that of soils in the most of the ChEs studied (Na, Al, Ca, Fe, and all the trace elements) due to the presence of effective physiological barriers in birch, as explained by the example above. Such barriers

accounted for its capability to grow on highly toxic substrates of the MBCB's spoil heaps and talus [26–28] where other plants could not survive. However, the concentration of Mg in birch leaves and branches was closely correlated with its content in exchangeable and specifically adsorbed fractions, as well as with the total content in soils, despite the insignificant correlation with water-soluble compounds. A similar trend was observed in P (Table S14). The S content in birch aerial tissues was significantly correlated with its extractability. The content of water-soluble compounds of K in soils was significantly ($r > 0.92$, $n = 8$) correlated with the K concentration in plants.

In the studied surface waters within the Moscow Brown Coal Basin, the content of Cu in all samples and Zn in the majority of samples was below their maximal permissible concentrations (MPCs) according to the Russian water quality standards for all kinds of aquatic systems (including drinking water reservoirs and subterranean and surface water bodies for agricultural and recreational uses). The content of Co, Fe, Mg, Mn, Ni, P, and Pb exceeded their MPCs in the majority of water samples from the mine sites (Table S13). This indicates that local rivers are at risk of water pollution via the mine drainage. In the surface water samples from the unpolluted site, the concentrations of Fe, Mn, P, and Pb exceeded their MPCs as well. This likely results from regional-scale water pollution, taking into account the fact that the study region has well-developed industry and agriculture [90].

The studied soils were less contaminated by inorganic pollutants compared to the surface waters. The concentration of total Ni, Pb, and Zn and the mobile fractions of Co, Mn, Ni, and Zn exceeded their MPCs in only 30% of the soil samples. The total S content exceeded its MPC in the absolute majority of soil samples, including those from the unpolluted site. This might be connected with both regional-scale soil pollution and the local properties of the studied Chernozems, where enrichment in certain elements could be natural, e.g., due to the high content of clay particles and total organic carbon.

The detected levels of potentially toxic elements are typical for soils and surface water affected by acid mine drainage [110]. We did not find very high content levels of the potentially toxic elements in surface water or soils, which is in line with the ability of plants to colonize the abandoned mining areas of the Moscow Brown Coal Basin. Observed bare ground soils may result from severe erosion and water deficiency in the soils of the spoil heap steep slopes, as well as sulfuric acid formation. In Spain [111], territories with similar environmental harshness were covered by shrubs (*Erica cinerea* L., *Ulex europaeus* L. and *Rubus fruticosus* L.). Greater environmental harshness (high acidity and/or higher content of toxic elements) was reported for territories affected by acid mine drainage in [112–119]. Unfortunately, these studies did not provide data on vegetation grown in Spolic Technosols and/or Spolic Regosols. These sites could have been bare ground and not revegetated during a long period, as previously reported in [120].

4. Conclusions

In the Moscow Brown Coal Basin, ecosystems affected by highly saline acid sulfate solutions were enriched in potentially toxic elements to levels much higher than their maximal permissible concentrations. The degrees of pollution decreased between the surface waters and soils, and further to plants, with generally decreasing pollution with increasing distance from spoil heaps.

The chemical composition of birch aerial tissues reflected a high adaptability of this tree species to the very acidic substrates enriched in potentially toxic elements in readily available chemical forms.

Soils buried under and formed on the talus mantles at the footslope of the abandoned spoil heaps could be regarded as geochemical barriers on the migration routes of potentially toxic elements, which accumulate at such barriers. However, this is correct just for elements in which extractability decreases compared with the A horizon of the Technosols and Regosols studied. Under the toeslope colluvial mantle, the A horizon of black soils was transformed into a depletion zone, while both the B and C horizons served as zones of accumulation of different substances.

Further research can be directed at an assessment of the spatial distribution of water pollution and soil contamination, which is particularly important in terms of water quality control to provide the local population with clean water for drinking, crop irrigation, and other needs.

Supplementary Materials: The following supporting information can be downloaded at: <https://www.mdpi.com/article/10.3390/w14010113/s1>, Figure S1: Chemical element speciation (average percentage) in the Spolic A-horizons studied; Table S1: Main morphological features of soils studied in the Kireevskii and Uzlovskii districts of the Tula region [26–28,39]; Table S2: The number of soil samples collected at the sites studied; Table S3: The number of surface water samples collected at the sites studied; Table S4: The root-mean-square deviation values (relative percentage, %) for the X-ray fluorescence data on the elemental composition of the soils studied; Table S5: Lower detection limits and the quality of the analysis and quality control for plant and water samples; Table S6: Lower detection limits (LDLs) and the quality of the analysis and quality control for liquid samples of soil extracts; Table S7: Characteristics ($m \pm SD$) of the studied surface waters sampled at the different locations; Table S8: The spatial differentiation of the studied surface waters; Table S9: Characteristics ($m \pm SD$) of the studied soil horizons; Table S10: Spatial differentiation of the horizons of Regosols on talus at the footslope of spoil heaps; Table S11: Characteristics ($m \pm SD$) of the studied aerial tissues of a birch; Table S12: Spatial differentiation of the chemical composition of the analyzed birch tissues; Table S13: A comparison of chemical element concentration in the studied surface waters and soils with the water and soil quality standards of the Russian Federation; Table S14: Correlation matrix for the elemental composition of topsoil and birch aerial tissues, $n = 8$.

Author Contributions: I.S., conceptualization, methodology, software, formal analysis, investigation, data curation, writing—original draft preparation, review and editing; visualization, field and laboratory work, supervision, project co-administration. A.S., conceptualization, methodology, writing—review and editing, field and laboratory work, supervision, project administration, funding acquisition. S.L., methodology, writing—review and editing, field and laboratory work. N.Y., data curation, field and laboratory work. A.K., visualization. G.K., software, visualization, writing—review and editing. T.K., conceptualization, methodology, writing—review and editing. All authors have read and agreed to the published version of the manuscript.

Funding: Field and chemical-analytical work was carried out within the framework of the RFBR project No. 20-35-70066. Interpretation of the results was supported by M. V. Lomonosov Moscow State University (the Interdisciplinary Scientific and Educational School of “Future Planet and Global Environmental Change” and project I.4. “Anthropogenic geochemical transformation of the components of landscapes”).

Data Availability Statement: The data presented in this study are available on request from the corresponding author.

Acknowledgments: We are grateful to our colleagues who assisted with the field work, namely: B.A. Ibragimova, A.S. Saifutdinov, V.V. Sharapov, and E.S. Starchikova; and with the laboratory work, namely: T.A. Serebrennikova (soil sample pre-treatment), L.V. Dobrydneva, B.A. Ibragimova, E.S. Starchikova, E.V. Terskaya (pH and electrical conductivity measurement; Lomonosov Moscow State University), V.K. Karandashev (AES-ICP and ICP-MS; the Institute of Microelectronics Technology and High Purity Materials, Russian Academy of Sciences), and A.I. Yakushev (XRF spectrometry; the Institute of Geology of Ore Deposits, Petrography, Mineralogy, and Geochemistry of the Russian Academy of Sciences). Plant samples were ground using equipment acquired with the funding of the RSF project No. 17-77-20072. The authors are grateful to I. Spiridonova and M. Hayes for help with the manuscript preparation.

Conflicts of Interest: The authors declare no conflict of interest.

References

1. Prakash, V.; Sinha, S.K.; Das, N.C.; Panigrahi, D.C. Sustainable mining metrics en route a coal mine case study. *J. Clean. Prod.* **2020**, *268*, 122122. [[CrossRef](#)]
2. Ashfaq, M.; Lal, M.H.; Moghal, A.A.B.; Murthy, V.R. Carbon Footprint Analysis of Coal Gangue in Geotechnical Engineering Applications. *Indian Geotech. J.* **2020**, *50*, 646–654. [[CrossRef](#)]

3. Robles-Arenas, V.M.; Rodríguez, R.; García, C.; Manteca, J.I.; Candela, L. Sulphide-mining impacts in the physical environment: Sierra de Cartagena-La Unión (SE Spain) case study. *Environ. Geol.* **2006**, *51*, 47–64. [CrossRef]
4. Kislitsyna, V.V.; Surzhikov, D.V.; Likontseva, Y.S.; Golikov, R.A.; Staiger, V.A. The impact of air pollution during the liquidation and recultivation of mine workings on health problems risk of the population in an industrial city. *Russ. J. Occup. Health Ind. Ecol.* **2021**, *61*, 197–201. [CrossRef]
5. Gao, J.; Guan, C.H.; Zhang, B. China's CH₄ emissions from coal mining: A review of current bottom-up inventories. *Sci. Total Environ.* **2020**, *725*, 138295. [CrossRef]
6. Kopytov, A.I.; Manakov, Y.A.; Kupriyanov, A.N. Coal mining and issued of ecosystem preservation in Kuzbass. *Ugol* **2017**, *3*, 72–77. [CrossRef]
7. Zenkov, I.V.; Nefedov, N.B.; Morin, A.S.; Kiryushina, E.V.; Vokin, V.N.; Veretenova, T.A.; Kondrashov, P.M.; Pavlova, P.L.; Brezhnev, R.V. Land remediation technology in the development of coal deposits in the Northern Regions of Russia. *Ugol* **2020**, *4*, 62–67. [CrossRef]
8. Li, Y.T.; Becquer, T.; Dai, J.; Quantin, C.; Benedetti, M.F. Ion activity and distribution of heavy metals in acid mine drainage polluted subtropical soils. *Environ. Pollut.* **2009**, *157*, 1249–1257. [CrossRef]
9. Arroyo, R.R.Y.; Siebe, C. Weathering of sulphide minerals and trace element speciation in tailings of various ages in the Guanajuato mining district, Mexico. *Catena* **2007**, *71*, 497–506. [CrossRef]
10. Lu, S.; Teng, Y.; Wang, Y.; Wu, J.; Wang, J. Research on the ecological risk of heavy metals in the soil around a Pb–Zn mine in the Huize County, China. *Chin. J. Geochem.* **2015**, *34*, 540–549. [CrossRef]
11. Leonard, R.; Zulfikar, R.; Stansbury, R. Coal mining and lung disease in the 21st century. *Curr. Opin. Pulm. Med.* **2020**, *26*, 135–141. [CrossRef]
12. Punia, A. Role of temperature, wind, and precipitation in heavy metal contamination at copper mines: A review. *Environ. Sci. Pollut. Res.* **2021**, *28*, 4056–4072. [CrossRef]
13. Anawar, H.M. Sustainable rehabilitation of mining waste and acid mine drainage using geochemistry, mine type, mineralogy, texture, ore extraction and climate knowledge. *J. Environ. Manag.* **2015**, *158*, 111–121. [CrossRef]
14. Niu, A.; Lin, C. Managing soils of environmental significance: A critical review. *J. Hazard. Mater.* **2021**, *417*, 125990. [CrossRef]
15. Semenkov, I.N.; Klink, G.V.; Lebedeva, M.P.; Krupskaya, V.V.; Chernov, M.S.; Dorzhieva, O.V.; Kazinskiy, M.T.; Sokolov, V.N.; Zavadskaya, A.V. The variability of soils and vegetation of hydrothermal fields in the Valley of Geysers at Kamchatka Peninsula. *Sci. Rep.* **2021**, *11*, 11077. [CrossRef]
16. Tarazanov, I.G.; Gubanov, D.A. Russia's coal industry performance for January–December, 2019. *Ugol* **2020**, *3*, 27–43. [CrossRef]
17. Gavrilenko, A.M. Ministry of Energy of the Russian Federation. Available online: <https://minenergo.gov.ru/node/433> (accessed on 24 December 2022).
18. Scripta Technica, Inc. Nina Petrovna Solntseva (1935–2004). *Eurasian Soil Sci.* **2005**, *38*, 792–793. Available online: [http://explore.bl.uk/primo_library/libweb/action/display.do?tabs=moreTab&ct=display&fn=search&doc=ETOCRN173423523&indx=1&recIds=ETOCRN173423523&recIdx=0&elementId=0&renderMode=poppedOut&displayMode=full&frbrVersion=&frbg=&dscent=0&vl\(2084770704UI0\)=any&scps=scope%3A%28BLCCONTENT%29&tb=t&vid=BLVU1&mode=Basic&srt=rank&tab=local_tab&dum=true&vl\(freeText0\)=nina%20Petrovna%20Solntseva%20%281935-2004%29&dstmp=1641310416353](http://explore.bl.uk/primo_library/libweb/action/display.do?tabs=moreTab&ct=display&fn=search&doc=ETOCRN173423523&indx=1&recIds=ETOCRN173423523&recIdx=0&elementId=0&renderMode=poppedOut&displayMode=full&frbrVersion=&frbg=&dscent=0&vl(2084770704UI0)=any&scps=scope%3A%28BLCCONTENT%29&tb=t&vid=BLVU1&mode=Basic&srt=rank&tab=local_tab&dum=true&vl(freeText0)=nina%20Petrovna%20Solntseva%20%281935-2004%29&dstmp=1641310416353) (accessed on 24 December 2022).
19. Solntseva, N.P. A system of geographical studies to conserve the quality of the environment (exemplified by the Moscow region). *Vestn.-Mosk. Univ. Seriya Geogr.* **1985**, *1*, 31–37.
20. Solntseva, N.P.; Rubilina, N.Y.; Gerasimova, M.I.; Alistratov, S.V. Alteration of the morphology of leached Chernozems in a coal-mining district. *Eurasian Soil Sci.* **1992**, *24*, 46–58.
21. Nikiforova, E.M.; Solntseva, N.P. Technogenic flows of sulphur in humid landscapes of coal-mining areas. *Vestn.-Mosk. Univ. Seriya Geogr.* **1986**, *3*, 52–59.
22. Perel'man, A.I. Geochemical barriers: Theory and practical applications. *Appl. Geochem.* **1986**, *1*, 669–680. [CrossRef]
23. Glazovskaya, M.A. Geochemical barriers in plain soils, their typology, functional characteristics and environmental importance. *Vestn. Mosk. Univ. Seriya 5 Geogr.* **2012**, *1*, 8–14.
24. Alekseenko, A.V. Geochemical Barriers for Soil Protection in Mining Areas. In *Assessment, Restoration and Reclamation of Mining Influenced Soils*; Bech, J., Bini, C., Pashkevich, M.A., Eds.; Elsevier Inc.: Amsterdam, The Netherlands, 2017; pp. 255–274, ISBN 9780128095881.
25. Sharapova, A.V.; Semenkov, I.N.; Lednev, S.A.; Karpachevsky, A.M.; Koroleva, T.V. Self-development of mining landscapes of the old coal mining district in tula region. *Ecol. Ind. Russ.* **2017**, *21*, 54–59. [CrossRef]
26. Sharapova, A.V.; Semenkov, I.N.; Lednev, S.A.; Karpachevsky, A.M.; Koroleva, T.V. Biochemical potential of self-development of post-technogenic mining-industrial geocomplexes of the Moscow coal basin. *Ugol* **2020**, *10*, 56–61. [CrossRef]
27. Lednev, S.A.; Sharapova, A.V.; Semenkov, I.N.; Kaepachevsky, A.M.; Koroleva, T.V. Plant successions on coal mines' waste piles in forest-steppe of the Tula oblast. *Izv. Ross. Akad. Nauk. Seriya Geogr.* **2020**, *84*, 239–245. [CrossRef]
28. Ahirwal, J.; Maiti, S.K.; Singh, A.K. Changes in ecosystem carbon pool and soil CO₂ flux following post-mine reclamation in dry tropical environment, India. *Sci. Total Environ.* **2017**, *583*, 153–162. [CrossRef]

29. Madejón, P.; Caro-Moreno, D.; Navarro-Fernández, C.M.; Rossini-Oliva, S.; Marañón, T. Rehabilitation of waste rock piles: Impact of acid drainage on potential toxicity by trace elements in plants and soil. *J. Environ. Manag.* **2021**, *280*, 111848. [[CrossRef](#)] [[PubMed](#)]
30. Chang Kee, J.; Gonzales, M.J.; Ponce, O.; Ramírez, L.; León, V.; Torres, A.; Corpus, M.; Loayza-Muro, R. Accumulation of heavy metals in native Andean plants: Potential tools for soil phytoremediation in Ancash (Peru). *Environ. Sci. Pollut. Res.* **2018**, *25*, 33957–33966. [[CrossRef](#)]
31. Karaca, O.; Comeselle, C.; Reddy, K.R. Mine tailing disposal sites: Contamination problems, remedial options and phytocaps for sustainable remediation. *Rev. Environ. Sci. Biotechnol.* **2018**, *17*, 205–228. [[CrossRef](#)]
32. Yang, S.X.; Liao, B.; Yang, Z.H.; Chai, L.Y.; Li, J.T. Revegetation of extremely acid mine soils based on aided phytostabilization: A case study from southern China. *Sci. Total Environ.* **2016**, *562*, 427–434. [[CrossRef](#)]
33. Krechetov, P.; Kostin, A.; Chernitsova, O.; Terskaya, E. Environmental changes due to wet disposal of wastes from coal-fired heat power plant: A case study from the Tula Region, Central Russia. *Appl. Geochem.* **2019**, *105*, 105–113. [[CrossRef](#)]
34. Krechetov, P.; Chernitsova, O.; Sharapova, A.; Terskaya, E. Technogenic geochemical evolution of chernozems in the sulfur coal mining areas. *J. Soils Sediments* **2019**, *19*, 3139–3154. [[CrossRef](#)]
35. Golosov, V.; Panin, A. Century-scale stream network dynamics in the Russian Plain in response to climate and land use change. *Catena* **2006**, *66*, 74–92. [[CrossRef](#)]
36. Peel, M.C.; Finlayson, B.L.; McMahon, T.A. Updated world map of the Köppen-Geiger climate classification. *Hydrol. Earth Syst. Sci.* **2007**, *11*, 1633–1644. [[CrossRef](#)]
37. Volkova, E.M.; Lebedeva, M.V.; Yamalov, S.M. Vegetation dynamics of Kulikovo Field agrostepes: The contribution of environmental factors. *IOP Conf. Ser. Earth Environ. Sci.* **2021**, *817*, 012112. [[CrossRef](#)]
38. Arkhipova, M.V. *The Current State of Deciduous Forests of the Central Russian Upland (Based on Cartographic Materials and Remote Sensing Data)*; Lomonosov Moscow State University: Moscow, Russia, 2014.
39. Sharapova, A.V.; Semenov, I.N.; Karpachevsky, A.M.; Lednev, S.A.; Koroleva, T.V. Morphological and chemical properties of soils within geological complexes affected by sulfuric acid in forest-steppe of the Central Russian Upland (Russia). In Proceedings of the IOP Conference Series: Earth and Environmental Science, The VIII Congress of the Dokuchaev Soil Science Society, Syktyvkar, Komi Republic, Russia, 19–24 July 2021; p. 012013.
40. FAO. *World Reference Base for Soil Resources 2014 International Soil Classification System*; FAO: Rome, Italy, 2015; ISBN 9789251083697.
41. FAO. *Guidelines for Soil Description*, 4th ed.; Food and Agriculture Organisation of the United Nations: Rome, Italy, 2006; ISBN 9251054908.
42. van Reeuwijk, L.P. *Procedures for Soil Analysis*, 3rd ed.; Reeuwijk, L.P., Ed.; ISRIC FAO: Wageningen, The Netherlands, 2002.
43. Minkina, T.M.; Mandzhieva, S.S.; Burachevskaya, M.V.; Bauer, T.V.; Sushkova, S.N. Method of determining loosely bound compounds of heavy metals in the soil. *MethodsX* **2018**, *5*, 217–226. [[CrossRef](#)] [[PubMed](#)]
44. Minkina, T.M.; Motuzova, G.V.; Nazarenko, O.G.; Kryshchenko, V.S.; Mandzhieva, S.S. Forms of heavy metal compounds in soils of the steppe zone. *Eurasian Soil Sci.* **2008**, *41*, 708–716. [[CrossRef](#)]
45. Semenov, I.N.; Koroleva, T.V. The spatial distribution of fractions and the total content of 24 chemical elements in soil catenas within a small gully's catchment area in the Trans Urals, Russia. *Appl. Geochem.* **2019**, *106*, 1–6. [[CrossRef](#)]
46. Ladonin, D.V. Heavy metal compounds in soils: Problems and methods of study. *Eurasian Soil Sci.* **2002**, *35*, 605–613.
47. Diatta, J.; Andrzejewska, A.; Rafałowicz, T. Reactivity, exchangeability and solubility of heavy metals in various soil materials—Concepts and evaluation. *Eurasian Soil Sci.* **2019**, *52*, 853–864. [[CrossRef](#)]
48. Solov'ev, G.A. The use of complex extracts to determine the available forms of trace elements in soils. In *Monitoring of Background Environmental Pollution*; Izrael, Y.A., Rovinsky, F.Y., Eds.; Gidrometeoizdat: Leningrad, Russia, 1989; pp. 216–227.
49. Minkina, T.M.; Motuzova, G.V.; Nazarenko, O.G.; Kryshchenko, V.S.; Mandzhieva, S.S. Combined approach for fractioning metal compounds in soils. *Eurasian Soil Sci.* **2008**, *41*, 1171–1179. [[CrossRef](#)]
50. Lee, P.K.; Kang, M.J.; Choi, S.H.; Touray, J.C. Sulfide oxidation and the natural attenuation of arsenic and trace metals in the waste rocks of the abandoned Seobo tungsten mine, Korea. *Appl. Geochem.* **2005**, *20*, 1687–1703. [[CrossRef](#)]
51. Vasil'eva, I.E.; Shabanova, E.V. *Catalogue of Certified Reference Materials of Natural and Man-Made Media Compositions*; A.P. Vinogradov Institute of Geochemistry SB RAS: Irkutsk, Russia, 2017.
52. Samczyński, Z.; Dybczyński, R.S.; Polkowska-Motrenko, H.; Chajduk, E.; Pyszynska, M.; Danko, B.; Czerska, E.; Kulisa, K.; Doner, K.; Kalbarczyk, P. Two new reference materials based on tobacco leaves: Certification for over a dozen of toxic and essential elements. *Sci. World J.* **2012**. [[CrossRef](#)]
53. Kasimov, N.S. Lateral migration of microelements in the steppe and desert landscapes. *Vestn. Mosk. Univ. Seriya Geogr.* **1981**, *5*, 69–74.
54. Kasimov, N.S.; Perel'man, A.I. The geochemistry of soils. *Eurasian Soil Sci.* **1992**, *24*, 59–76.
55. Polynov, B.B. *The Cycle of Weathering*; T. Murby & Co: London, UK, 1937.
56. Kovalevskii, A.L. Biogeochemical prospecting for ore deposits in the U.S.S.R. *J. Geochem. Explor.* **1984**, *21*, 63–72. [[CrossRef](#)]
57. Glazovskaya, M.A.; Kasimov, N.S. Landscape geochemical foundations of background monitoring of environment. *Vestn.-Mosk. Univ. Seriya Geogr.* **1987**, *1*, 11–17.
58. Kabata-Pendias, A.; Szteke, B. *Trace Elements in Abiotic and Biotic Environments*; CRC Press: Boca Raton, FL, USA; Taylor & Francis Group: London, UK; New York, NY, USA, 2015; ISBN 9781482212815.

59. Vozhdaeva, M.Y.; Kholova, A.R.; Vagner, E.V.; Trukhanova, N.V.; Melnitskiy, I.A.; Mullodzhanov, T.T.; Kantor, E.A. Changes in the indicators of chemical safety of drinking water in Ufa during its transportation to consumers. *Gig. Sanit.* **2021**, *100*, 396–405. [[CrossRef](#)]
60. Koroleva, T.V.; Semenov, I.N.; Sharapova, A.V.; Krechetov, P.P.; Lednev, S.A. Ecological consequences of space rocket accidents in Kazakhstan between 1999 and 2018. *Environ. Pollut.* **2021**, *268*, 115711. [[CrossRef](#)] [[PubMed](#)]
61. Semenov, I.N.; Koroleva, T.V. International environmental regulation of chemical element content in soils: Guidelines and schemes. *Eurasian Soil Sci.* **2019**, *52*, 1289–1297. [[CrossRef](#)]
62. Semenov, I.N.; Koroleva, T.V. Guideline Values for the Content of Chemical Elements in Soils of Functional Zones at Cities (Review). *Eurasian Soil Sci.* **2022**, *55*, in press.
63. Gałuszka, A.; Migaszewski, Z.M.; Pelc, A.; Trembaczowski, A.; Dołęgowska, S.; Michalik, A. Trace elements and stable sulfur isotopes in plants of acid mine drainage area: Implications for revegetation of degraded land. *J. Environ. Sci.* **2020**, *94*, 128–136. [[CrossRef](#)]
64. Semenov, I.N.; Kasimov, N.S.; Terskaya, E.V. Vertical geochemical structure of soils of the forest-steppe loamy catenas of a balka water catchment in the centre of the Srednerusskaya upland. *Vestn. Mosk. Univ. Seriya 5 Geogr.* **2015**, *5*, 42–53.
65. Semenov, I.N.; Aseeva, E.N.; Terskaya, E.V. Geochemical structure of forest-steppe catenas of a balka drainage area in the Upa River basin. *Vestn. Mosk. Univ. Seriya 5 Geogr.* **2013**, *6*, 68–75.
66. Shcheglov, D.I.; Gorbunova, N.S.; Semenova, L.A.; Khatutseva, O.A. Microelements in soils of conjugated landscapes with different degrees of hydromorphism in the Kamennaya steppe. *Eurasian Soil Sci.* **2013**, *46*, 254–261. [[CrossRef](#)]
67. Dubovik, D.V.; Dubovik, E.V. Heavy metals in ordinary chernozems on slopes of different gradients and aspects. *Eurasian Soil Sci.* **2016**, *49*, 33–44. [[CrossRef](#)]
68. Protasova, N.A.; Shcherbakov, A.P. Microelemental composition of zonal soils in the central chernozemic region. *Eurasian Soil Sci.* **2004**, *37*, 40–48.
69. Lisetskii, F.; Stolba, V.F.; Marinina, O. Indicators of agricultural soil genesis under varying conditions of land use, Steppe Crimea. *Geoderma* **2015**, 239–240, 304–316. [[CrossRef](#)]
70. Solntseva, N.P.; Gerasimova, M.I.; Rubilina, N.Y. Morphogenetic analysis of soils transformed by technology. *Sov. Soil Sci.* **1991**, *23*, 87–94.
71. Bazykina, G.S.; Ovechkin, S.V. The influence of climate cycles on the water regime and carbonate profile in chernozems of Central European Russia and adjacent territories. *Eurasian Soil Sci.* **2016**, *49*, 437–449. [[CrossRef](#)]
72. Goryachkin, S.V.; Tonkonogov, V.D.; Gerasimova, M.I.; Lebedeva, I.I.; Shishov, L.L.; Targulian, V.O. Changing Concepts of Soil and Soil Classification in Russia. In *Soil Classification*; CRC Press: Boca Raton, FL, USA, 2019; pp. 187–199, ISBN 9780429125386.
73. Rozhkov, V.A. Soils and the soil cover as witnesses and indicators of global climate change. *Eurasian Soil Sci.* **2009**, *42*, 118–128. [[CrossRef](#)]
74. Lebedeva, I.I.; Tonkonogov, V.D.; Gerasimova, M.J. Geographical aspects of soil memory in mesomorphic soils of some Eurasian regions. *Eurasian Soil Sci.* **2002**, *35*, 30–41.
75. Lin, Z.; Herbert, R.B. Heavy metal retention in secondary precipitates from a mine rock dump and underlying soil, Dalarna, Sweden. *Environ. Geol.* **1997**, *33*, 1–12. [[CrossRef](#)]
76. Salisbury, A.B.; Reinfelder, J.R.; Gallagher, F.J.; Grabosky, J.C. Long-term stability of trace element concentrations in a spontaneously vegetated urban brownfield with anthropogenic soils. *Soil Sci.* **2017**, *182*, 69–81. [[CrossRef](#)]
77. Gennadiev, A.N.; Geptner, A.R.; Zhidkin, A.P.; Chernyanskiy, S.S.; Pikovskii, Y.I. Exothermic and endothermic soils of Iceland. *Eurasian Soil Sci.* **2007**, *40*, 595–607. [[CrossRef](#)]
78. Gol'dfarb, I.L. Effect of hydrothermal activity on the conditions of pedogenesis and soil morphology (by the example of Kamchatka). *Eurasian Soil Sci.* **1996**, *29*, 1319–1324.
79. Kostyuk, D.N.; Gennadiev, A.N. Soils and the soil cover of the Valley of Geysers. *Eurasian Soil Sci.* **2014**, *47*, 529–539. [[CrossRef](#)]
80. Othmani, M.A.; Souissi, F.; Durães, N.; Abdelkader, M.; da Silva, E.F. Assessment of metal pollution in a former mining area in the NW Tunisia: Spatial distribution and fraction of Cd, Pb and Zn in soil. *Environ. Monit. Assess.* **2015**, *187*, 523. [[CrossRef](#)]
81. Sommer, M.; Schlichting, E. Archetypes of catenas in respect to matter a concept for structuring and grouping catenas. *Geoderma* **1997**, *76*, 1–33. [[CrossRef](#)]
82. Semenov, I.N.; Kasimov, N.S.; Terskaya, E.V. Lateral distribution of metal forms in tundra, taiga and forest steppe catenae of the east European plain. *Vestn. Mosk. Univ. Seriya 5 Geogr.* **2016**, *3*, 29–39.
83. Semenov, I.; Konyushkova, M. Geochemical partition of chemical elements in Kastanozems and Solonetz in a local catchment within a semiarid landscape of SW Russia. *Catena* **2022**, *210*, 105869. [[CrossRef](#)]
84. Herbert, R.B. Partitioning of heavy metals in podzol soils contaminated by mine drainage waters, Dalarna, Sweden. *Water Air Soil Pollut.* **1997**, *96*, 39–59. [[CrossRef](#)]
85. Armienta, M.A.; Mugica, V.; Reséndiz, I.; Arzaluz, M.G. Arsenic and metals mobility in soils impacted by tailings at Zimapán, México. *J. Soils Sediments* **2016**, *16*, 1267–1278. [[CrossRef](#)]
86. Kasimov, N.S.; Samonova, O.A.; Aseeva, E.N. Background soil-geochemical structure of Privolzhskaya upland forest-steppe. *Pochvovedenie* **1992**, *8*, 5–21.
87. Semenov, I.; Yakushev, A. Dataset on heavy metal content in background soils of the three gully catchments at Western Siberia. *Data Br.* **2019**, *26*, 104496. [[CrossRef](#)]

88. Semenkov, I.; Krupskaya, V.; Klink, G. Data on the concentration of fractions and the total content of chemical elements in catenae within a small catchment area in the Trans Urals, Russia. *Data Br.* **2019**, *25*, 104224. [[CrossRef](#)]
89. Yang, S.X.; Liao, B.; Li, J.T.; Guo, T.; Shu, W.S. Acidification, heavy metal mobility and nutrient accumulation in the soil-plant system of a revegetated acid mine wasteland. *Chemosphere* **2010**, *80*, 852–859. [[CrossRef](#)] [[PubMed](#)]
90. Shopina, O.V.; Semenkov, I.N.; Paramonova, T.A. The accumulation of heavy metals and ¹³⁷Cs in plant products grown on radioactively contaminated chernozems of Tula oblast. *Ecol. Ind. Russ.* **2020**, *24*, 48–53. [[CrossRef](#)]
91. Rajput, V.; Minkina, T.; Semenkov, I.; Klink, G.; Tarigholizadeh, S.; Sushkova, S. Phylogenetic analysis of hyperaccumulator plant species for heavy metals and polycyclic aromatic hydrocarbons. *Environ. Geochem. Health* **2021**, *43*, 1629–1654. [[CrossRef](#)]
92. Mleczek, M.; Goliński, P.; Krzesłowska, M.; Gąsecka, M.; Magdziak, Z.; Rutkowski, P.; Budzyńska, S.; Waliszewska, B.; Kozubik, T.; Karolewski, Z.; et al. Phytoextraction of potentially toxic elements by six tree species growing on hazardous mining sludge. *Environ. Sci. Pollut. Res.* **2017**, *24*, 22183–22195. [[CrossRef](#)]
93. Alam, M.R.; Islam, R.; Anh Tran, T.K.; Van, D.L.; Rahman, M.M.; Griffin, A.S.; Yu, R.M.K.; MacFarlane, G.R. Global patterns of accumulation and partitioning of metals in halophytic saltmarsh taxa: A phylogenetic comparative approach. *J. Hazard. Mater.* **2021**, *414*, 125515. [[CrossRef](#)]
94. Martins, M.; Faleiro, M.L.; Barros, R.J.; Veríssimo, A.R.; Barreiros, M.A.; Costa, M.C. Characterization and activity studies of highly heavy metal resistant sulphate-reducing bacteria to be used in acid mine drainage decontamination. *J. Hazard. Mater.* **2009**, *166*, 706–713. [[CrossRef](#)]
95. Kasimov, N.S.; Lychagin, M.Y.; Chalov, R.S.; Shinkareva, G.L. Paragenetic associations of chemical elements in landscapes. *Vestn. Mosk. Univ. Seriya 5 Geogr.* **2019**, *6*, 20–28.
96. Gagnon, V.; Rodrigue-Morin, M.; Tardif, A.; Beaudin, J.; Greer, C.W.; Shipley, B.; Bellenger, J.P.; Roy, S. Differences in elemental composition of tailings, soils, and plant tissues following five decades of native plant colonization on a gold mine site in Northwestern Québec. *Chemosphere* **2020**, *250*, 126243. [[CrossRef](#)]
97. Alvarenga, P.; Simões, I.; Palma, P.; Amaral, O.; Matos, J.X. Field study on the accumulation of trace elements by vegetables produced in the vicinity of abandoned pyrite mines. *Sci. Total Environ.* **2014**, *470–471*, 1233–1242. [[CrossRef](#)]
98. Perlatti, F.; Ferreira, T.O.; da Costa Roberto, F.A.; Romero, R.E.; Sartor, L.R.; Otero, X.L. Trace metal/metalloid concentrations in waste rock, soils and spontaneous plants in the surroundings of an abandoned mine in semi-arid NE-Brazil. *Environ. Earth Sci.* **2015**, *74*, 5427–5441. [[CrossRef](#)]
99. Bartuska, A.M.; Ungar, I.A. Elemental concentrations in plant tissues as influenced by low pH soils. *Plant Soil* **1980**, *55*, 157–161. [[CrossRef](#)]
100. Durães, N.; Bobos, I.; Ferreira da Silva, E.; Dekayir, A. Copper, zinc and lead biogeochemistry in aquatic and land plants from the Iberian Pyrite Belt (Portugal) and north of Morocco mining areas. *Environ. Sci. Pollut. Res.* **2015**, *22*, 2087–2105. [[CrossRef](#)]
101. Santos, E.S.; Abreu, M.M.; Nabais, C.; Magalhães, M.C.F. Trace element distribution in soils developed on gossan mine wastes and *Cistus ladanifer* L. tolerance and bioaccumulation. *J. Geochem. Explor.* **2012**, *123*, 45–51. [[CrossRef](#)]
102. Alekseenko, V.A.; Bech, J.; Alekseenko, A.V.; Shvydkaya, N.V.; Roca, N. Environmental impact of disposal of coal mining wastes on soils and plants in Rostov Oblast, Russia. *J. Geochem. Explor.* **2018**, *184*, 261–270. [[CrossRef](#)]
103. Luo, L.; Chu, B.; Liu, Y.; Wang, X.; Xu, T.; Bo, Y. Distribution, origin, and transformation of metal and metalloid pollution in vegetable fields, irrigation water, and aerosols near a Pb-Zn mine. *Environ. Sci. Pollut. Res.* **2014**, *21*, 8242–8260. [[CrossRef](#)] [[PubMed](#)]
104. Li, F.; Li, X.; Hou, L.; Shao, A. Impact of the Coal Mining on the Spatial Distribution of Potentially Toxic Metals in Farmland Tillage Soil. *Sci. Rep.* **2018**, *8*, 14925. [[CrossRef](#)]
105. Solntseva, N.P. Trends in soil evolution under technogenic impacts. *Eurasian Soil Sci.* **2002**, *35*, 6–16.
106. Punanova, S.A.; Shpirt, M.Y. Ecological Consequences of the Development of Shale Formations Containing Toxic Elements. *Solid Fuel Chem.* **2018**, *52*, 396–405. [[CrossRef](#)]
107. Kasimov, N.S.; Gavrilova, I.P.; Gerasimova, M.I.; Bogdanova, M.D. New landscapes for resource-oriented geographical investigations. *Vestn. Mosk. Univ. Seriya 5 Geogr.* **2009**, *1*, 30–37.
108. Abdrakhmanov, R.F.; Akhmetov, R.M. Hydrogeochemistry at mining districts. *Geochem. Int.* **2016**, *54*, 795–806. [[CrossRef](#)]
109. Yang, C.; Lu, G.; Chen, M.; Xie, Y.; Guo, C.; Reinfelder, J.; Yi, X.; Wang, H.; Dang, Z. Spatial and temporal distributions of sulfur species in paddy soils affected by acid mine drainage in Dabaoshan sulfide mining area, South China. *Geoderma* **2016**, *281*, 21–29. [[CrossRef](#)]
110. Perotti, M.; Petrini, R.; D’Orazio, M.; Ghezzi, L.; Giannechini, R.; Vezzoni, S. Thallium and Other Potentially Toxic Elements in the Baccatoio Stream Catchment (Northern Tuscany, Italy) Receiving Drainages from Abandoned Mines. *Mine Water Environ.* **2018**, *37*, 431–441. [[CrossRef](#)]
111. Lago-Vila, M.; Arenas-Lago, D.; Andrade, L.; Vega, F.A. Phytoavailable content of metals in soils from copper mine tailings (Touro mine, Galicia, Spain). *J. Geochem. Explor.* **2014**, *147*, 159–166. [[CrossRef](#)]
112. Sahoo, P.K.; Tripathy, S.; Panigrahi, M.K.; Equeenuddin, S.M. Geochemical characterization of coal and waste rocks from a high sulfur bearing coalfield, India: Implication for acid and metal generation. *J. Geochem. Explor.* **2014**, *145*, 135–147. [[CrossRef](#)]
113. Álvarez-Valero, A.M.; Sáez, R.; Pérez-López, R.; Delgado, J.; Nieto, J.M. Evaluation of heavy metal bio-availability from Almagrera pyrite-rich tailings dam (Iberian Pyrite Belt, SW Spain) based on a sequential extraction procedure. *J. Geochem. Explor.* **2009**, *102*, 87–94. [[CrossRef](#)]

114. Maia, F.; Pinto, C.; Waerenborgh, J.C.; Gonçalves, M.A.; Prazeres, C.; Carreira, O.; Sério, S. Metal partitioning in sediments and mineralogical controls on the acid mine drainage in Ribeira da água Forte (Aljustrel, Iberian Pyrite Belt, Southern Portugal). *Appl. Geochem.* **2012**, *27*, 1063–1080. [[CrossRef](#)]
115. García-Lorenzo, M.L.; Pérez-Sirvent, C.; Molina-Ruiz, J.; Martínez-Sánchez, M.J. Mobility indices for the assessment of metal contamination in soils affected by old mining activities. *J. Geochem. Explor.* **2014**, *147*, 117–129. [[CrossRef](#)]
116. Pérez-López, R.; Álvarez-Valero, A.M.; Nieto, J.M.; Sáez, R.; Matos, J.X. Use of sequential extraction procedure for assessing the environmental impact at regional scale of the São Domingos Mine (Iberian Pyrite Belt). *Appl. Geochem.* **2008**, *23*, 3452–3463. [[CrossRef](#)]
117. Romero, F.M.; Prol-Ledesma, R.M.; Canet, C.; Alvares, L.N.; Pérez-Vázquez, R. Acid drainage at the inactive Santa Lucia mine, western Cuba: Natural attenuation of arsenic, barium and lead, and geochemical behavior of rare earth elements. *Appl. Geochem.* **2010**, *25*, 716–727. [[CrossRef](#)]
118. Montes-Avila, I.; Espinosa-Serrano, E.; Castro-Larragoitia, J.; Lázaro, I.; Cardona, A. Chemical mobility of inorganic elements in stream sediments of a semiarid zone impacted by ancient mine residues. *Appl. Geochem.* **2019**, *100*, 8–21. [[CrossRef](#)]
119. Andráš, P.; Midula, P.; Matos, J.X.; Buccheri, G.; Drímal, M.L.; Dirner, V.; Melichová, Z.; Turisová, I. Comparison of Soil Contamination at the Selected European Copper Mines. *Carpathian J. Earth Environ. Sci.* **2021**, *16*, 163–174. [[CrossRef](#)]
120. Grieco, G.; Sinojmeri, A.; Bussolesi, M.; Cocomazzi, G.; Cavallo, A. Environmental impact variability of copper tailing dumps in fushe arrez (Northern albania): The role of pyrite separation during flotation. *Sustainability* **2021**, *13*, 9643. [[CrossRef](#)]